AD-A162 276 THE MOTION OF A PUSHED SLIDING OBJECT PART 1 SLIDING FRICTION(U) CARNEGIE-MELLON UNIV PITTSBURGH PA ROBOTICS INST M A PESHKIN ET AL. SEP 85 CMU-RI-TR-85-18-PT-1 1/1

UNCLASSIFIED F/G 20/11 NL

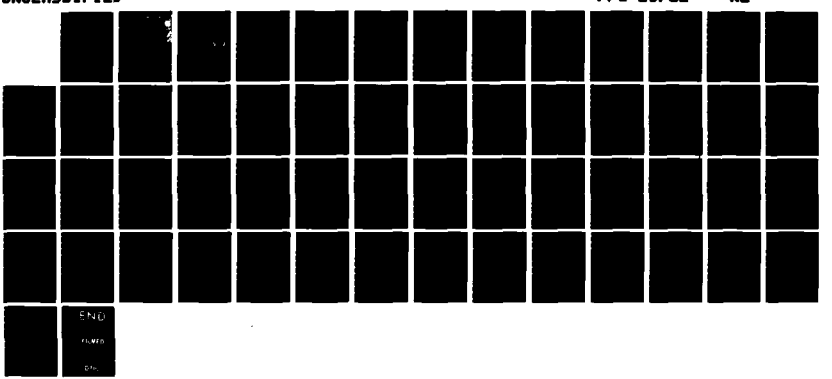

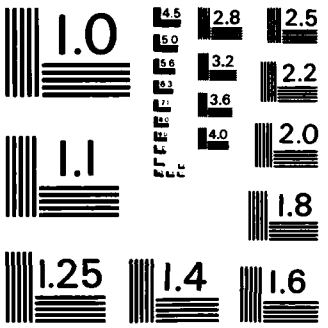

MICROCOPY RESOLUTION TEST CHART
NATIONAL BUREAU OF STANDARDS - 1963 - A

(12)

The Motion of a Pushed, Sliding Object
Part 1: Sliding Friction

M. A. Peshkin and A. C. Sanderson

CMU-RI-TR-85-18

Carnegie-Mellon University
The Robotics Institute

Technical Report

(12)

The Motion of a Pushed, Sliding Object
Part 1: Sliding Friction

M. A. Peshkin and A. C. Sanderson

CMU-RI-TR-85-18

The Robotics Institute
Carnegie-Mellon University
Pittsburgh, Pennsylvania 15213

September 1985

This work was supported by a grant from Xerox Corporation, and by the Robotics Institute, Carnegie-Mellon University.

Unclassified
SECURITY CLASSIFICATION OF THIS PAGE (When Data Entered)

REPORT DOCUMENTATION PAGE		READ INSTRUCTIONS BEFORE COMPLETING FORM
1. REPORT NUMBER CMU-RI-TR-85-18	2. GOVT ACCESSION NO. AD-A162276	3. RECIPIENT'S CATALOG NUMBER
4. TITLE (and Subtitle) The Motion of a Pushed, Sliding Object Part I: Sliding Friction		5. TYPE OF REPORT & PERIOD COVERED Interim 6. PERFORMING ORG. REPORT NUMBER
7. AUTHOR(s) M. A. Peshkin and A. C. Sanderson		8. CONTRACT OR GRANT NUMBER(s)
9. PERFORMING ORGANIZATION NAME AND ADDRESS Carnegie-Mellon University The Robotics Institute Pittsburgh, PA. 15213		10. PROGRAM ELEMENT, PROJECT, TASK AREA & WORK UNIT NUMBERS
11. CONTROLLING OFFICE NAME AND ADDRESS		12. REPORT DATE September 1985 13. NUMBER OF PAGES 48
14. MONITORING AGENCY NAME & ADDRESS(if different from Controlling Office)		15. SECURITY CLASS. (of this report) UNCLASSIFIED 15a. DECLASSIFICATION/DOWNGRADING SCHEDULE

16. DISTRIBUTION STATEMENT (of this Report)

Approved for public release; distribution unlimited

17. DISTRIBUTION STATEMENT (of the abstract entered in Block 20, if different from Report)

Approved for public release; distribution unlimited

18. SUPPLEMENTARY NOTES

19. KEY WORDS (Continue on reverse side if necessary and identify by block number)

20. ABSTRACT (Continue on reverse side if necessary and identify by block number)

In many robotic applications, manipulation planning for an object free to slide on a surface is an important problem. Physical analysis of the object's motion is made difficult by the absence of information about the distribution of support of the object, and of the resulting frictional forces. This paper describes a new approach to the analysis of sliding motion.

The instantaneous motion of the object can be described as a pure rotation about a center of rotation (COR) somewhere in the plane. In this paper we find the locus of CORs for all possible distributions of support forces. We assume zero friction—

DD FORM 1 JAN 73 1473 EDITION OF 1 NOV 65 IS OBSOLETE
S/N 0102-014-6601

UNCLASSIFIED
SECURITY CLASSIFICATION OF THIS PAGE (When Data Entered)

(20. cont'd)

at the pusher-object contact, and we assume that the support force distribution is confined to a disk.

In one application to robotic manipulation, bounds on the distance an object must be pushed to come into alighment with a robot finger or a fence are determined.

Table of Contents

1. Background 1
2. Overview 5
   2.1. The Center of Rotation 5
   2.2. The Support Distribution 7
   2.3. Overview 8
   2.4. Notation 10
3. Minimizing the Energy 12
   3.1. Relation between Motion of Pusher and Rotation of Object 12
   3.2. Energy Lost to Friction with the Table 14
   3.3. Iterative Numerical Solution 15
4. The Quotient Locus 16
   4.1. Extrema of the Quotient Locus 17
   4.2. Numerical Solution for the Quotient Locus 20
   4.3. Boundary for $|COR| < a$ 20
   4.4. Boundary for $|COR| > a$ 24
5. The COR Locus 26
   5.1. $|COR| < a$ 31
      5.1.1. Extremal Radius of the COR Locus Boundary for $|COR| < a$ 32
      5.1.2. Curvature of the COR Locus Boundary at r_{min} 32
   5.2. $|COR| > a$ 34
      5.2.1. Tip Line 34
      5.2.2. Curvature of the COR Locus Bound at the Tip 36
   5.3. Summary 38
6. Applications 38
7. Conclusion 45
8. Acknowledgements 45
9. Appendix - Validity of Energy Minimization 45

List of Figures

Figure 1-1: Hinge grasp strategy 3
Figure 1-2: The fence must advance 2.02 inches to assure that the rectangle is aligned 4
Figure 2-1: An object being pushed has two degrees of freedom 6
Figure 2-2: Parameters of the pushing problem 9
Figure 2-3: COR locus found by iterative minimization (dots) 11
Figure 3-1: Relation between advance of pusher (δx) and rotation about the COR ($\delta\theta$) 13
Figure 4-1: Dipod responsible for the smallest value of $\vec{v}_r$, for $r > a$ 18
Figure 4-2: Dipod responsible for a negative value of $\vec{v}_r$, for $r < a$ 19
Figure 4-3: Quotient locus $\{\vec{q}_r\}$ (dots), and empirical boundary (solid), for $r < a$ 21
Figure 4-4: Quotient locus $\{\vec{q}_r\}$ (dots), and empirical boundary (solid), for $r > a$ 22
Figure 4-5: Dipods contributing to the boundary of $\{\vec{q}_r\}$, for $r < a$ 23
Figure 4-6: Dipods contributing to the boundary of $\{\vec{q}_r\}$, for $r > a$ 25
Figure 5-1: Boundaries of quotient loci $\{\vec{q}_r\}$ for various $\vec{r}$ 27
Figure 5-2: Variables of equation 23, for a value of $\vec{r}$ not in the COR locus 28
Figure 5-3: Variables of equation 23, for a value of $\vec{r}$ in the COR locus 29
Figure 5-4: Variables of equation 23, for a value of $\vec{r}$ on the boundary of the COR locus 30
Figure 5-5: COR locus boundary for $r < a$ 33
Figure 5-6: Boundaries of COR loci for various $\vec{c}$ and α 35
Figure 5-7: $r_{tip}(\alpha)$ vs. α, and construction of the tip line 37
Figure 6-1: Initial configuration of object and fence, and resulting COR locus 40
Figure 6-2: Final configuration of object and fence, and resulting COR locus 41
Figure 6-3: y_{approx} is the distance from the line of motion to the tip of the COR locus 42
Figure 6-4: y_{true} is a bound for the distance from the line of motion to the true lowest point 44

Abstract

In many robotic applications, manipulation planning for an object free to slide on a surface is an important problem. Physical analysis of the object's motion is made difficult by the absence of information about the distribution of support of the object, and of the resulting frictional forces. This paper describes a new approach to the analysis of sliding motion.

The instantaneous motion of the object can be described as a pure rotation about a center of rotation (COR) somewhere in the plane. In this paper we find the locus of CORs for all possible distributions of support forces. We assume zero friction at the pusher-object contact, and we assume that the support force distribution is confined to a disk.

In one application to robotic manipulation, bounds on the distance an object must be pushed to come into alignment with a robot finger or a fence are determined.

1. Background

Sliding operations are encountered in several facets of robotics. It is almost inevitable that when the position of an object that is to be acquired by a robot is not perfectly known, a sliding phase will occur before the robot can acquire the object. This phase need not be considered an undesirable but unavoidable fact of life. The examples which follow show how sliding operations can be used constructively to manipulate and acquire objects, without sensing, and despite uncertainty in the orientation and position of the object. In each example, properties of sliding are used to reduce the uncertainty in position and orientation of an object.

In a typical grasping operation, the robot opens a two-jaw gripper wide enough to accommodate both the object to be grasped, and any uncertainty in the object's position. Then the gripper closes. If the object happens to be exactly centered between the jaws initially, both jaws will make contact the object simultaneously, and there will be no sliding phase. But this is unlikely. Usually, the object will be closer initially to one jaw than to the other, and the closer jaw will make contact first.

There follows a sliding phase until the second jaw makes contact. During the sliding phase the object is likely to rotate, especially if the face of the jaw is in contact with a corner of the object rather than a flat facet. Once both jaws come into contact with the object, sliding on the table becomes less important than *slipping* of the object with respect to the faces of the jaws. The behavior of an object during both phases is discussed in (Brost, 1985). Brost finds grasp strategies which bring the object into a unique configuration in the gripper, despite substantial uncertainty in its initial configuration.

Another example of the use of sliding is the interaction of an object on a moving belt with a fixed, slanted, fence across the belt. (Equivalently, the object may be stationary on a surface and the fence moving, under control of a robot.) One of many possible behaviors of the object when it hits the fence is to rotate until a flat edge is flush against the fence, and then to slide along the fence (if the fence is sufficiently slanted) until it reaches an obstruction at an edge of the belt. Another behavior is to roll along the fence instead of sliding. Or it may stop rotating and simply stick to the fence.

The behavior of objects on encountering a fence has been considered in (Mani, 1985) and (Brost, 1985). In (Mani, 1985), strategies for manipulation are developed which can orient an object on a table by pushing it in various directions with a fence. Each push aligns a facet of the object with the fence.

Bowl feeders, too, rely on sliding operations, as parts interact with fences while they move along a

ramp.

R. P. Paul demonstrated a clever grasping sequence on a hinge plate, illustrated in figure 1-1. The strategy makes use of sliding to simultaneously reduce the uncertainty of a hinge plate's configuration to zero, and then to grasp it (Paul, 1974) (Mason, 1985). To understand this and similar operations, Mason determined the conditions required for translation, clockwise (CW) rotation, and counter-clockwise (CCW) rotation of a pushed object (Mason, 1985). Mason's results are used extensively in both (Mani, 1985) and (Brost, 1985), and also in this work.

All of the work discussed above may be called "qualitative" in the best sense of that term: the authors find the exact conditions determining which of various qualitatively different behaviors will occur. The behavior in question may be that of rolling along a fence vs. slipping along a fence, or it may be that of rotating CCW vs. rotating CW as an object is pushed.

The work presented here is complementary to the work discussed above. One result of this work is quantitative bounds on the *rate* at which the predicted motion occurs. Without rate information the algorithms found in (Mani, 1985) cannot produce guaranteed manipulation strategies. In some cases, an object may have to be pushed a great distance before it will align with the fence pushing it. To produce a guaranteed strategy we need an upper bound on the distance an object must be pushed to align.

Brost's work is less dependent on rate information because the second phase (slipping relative to the jaws) is relatively insensitive to the interaction with the table (sliding). However certain of the grasp strategies analyzed in (Brost, 1985) do rely on sliding. Since pushing distances are finite these strategies can only be guaranteed if rotation rates are known.

Mason and Paul's hinge grasp (figure 1-1) works only for a certain range of initial hinge orientations. For orientations outside of this range, the jaws will be closing too fast for the hinge plate to complete its CW rotation into alignment, before the jaws close. To find the range of orientations for which this grasp will work, for a given convergence angle of the jaws, we need to know the slowest possible rotation rate of the hinge plate as it is pushed.

Figure 1-2 illustrates an application of the results of the present work. In the figure, a fence is pushing a rectangular object, which may slide on the table. The rectangle will rotate clockwise (CW) (Mason, 1985), and will cease to rotate when the long side becomes parallel to the fence (Brost, 1985) (Mani, 1985). So we can orient the rectangle by pushing it in this way. But how far do we have to push it?

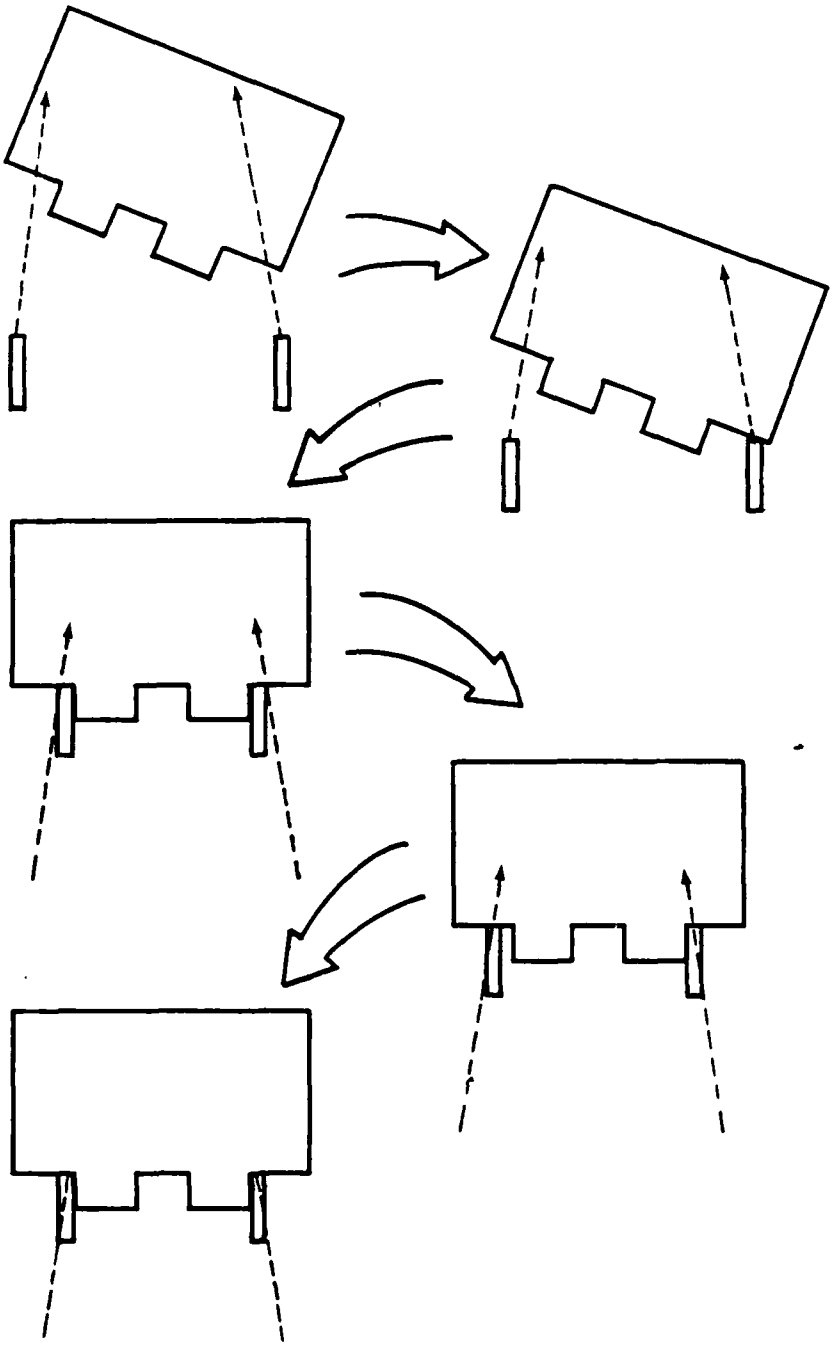

Figure 1-1: Hinge grasp strategy

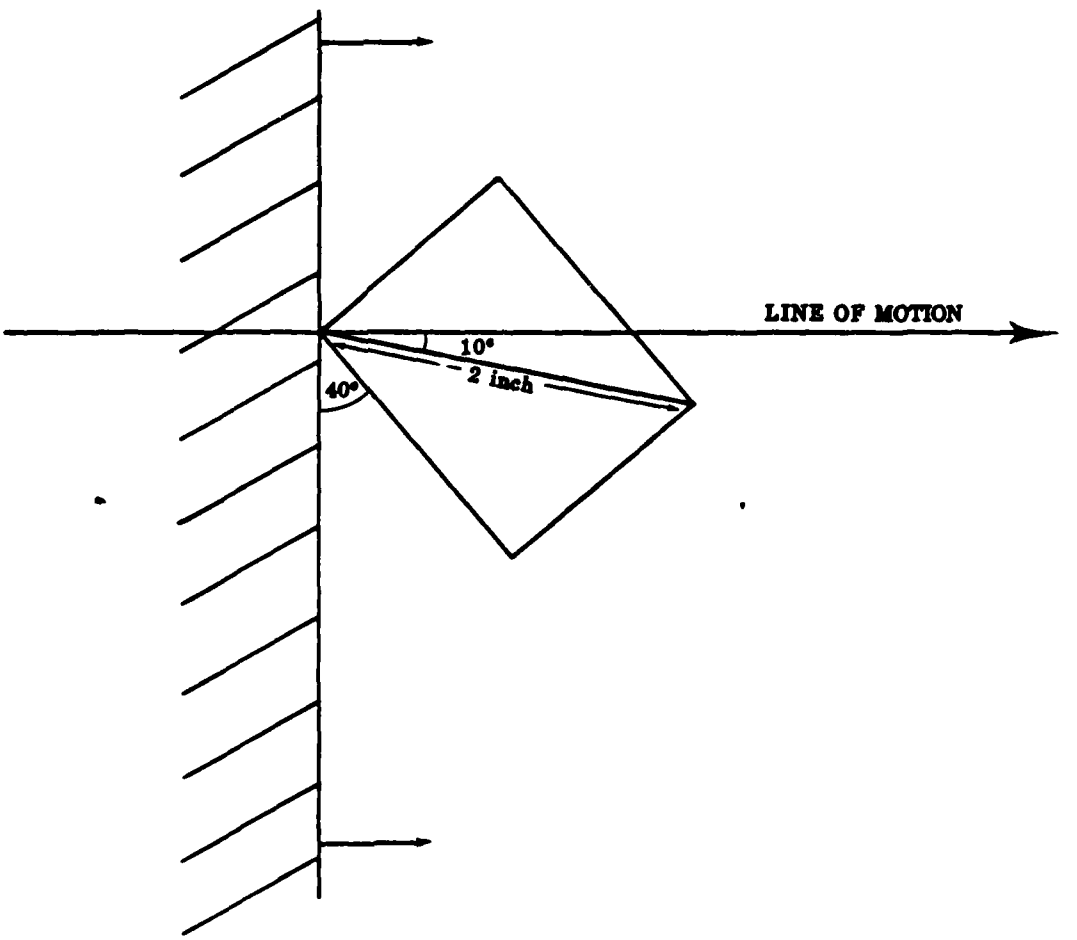

Figure 1-2: The fence must advance 2.02 inches to assure that the rectangle is aligned

In the example shown, we must push at most 2.02 inches to assure alignment. This result is independent of the mass of the object, the coefficient of friction between the object and the table, and of details of the bottom surface of the object (e.g., screw heads, cut-out sections, etc.). However it depends on the assumption that the coefficient of friction between the pusher and the object is zero.

2. Overview

2.1. The Center of Rotation

An object sliding on a plane has three degrees of freedom. Its position may be specified by the (x,y) displacement and angle θ of a coordinate frame fixed in the object relative to a coordinate frame fixed in the plane. The instantaneous motion of the object may be described as infinitesimal changes in the displacements and rotation.

In this paper we will treat the object as a two-dimensional rigid body, since we are only concerned with the interaction of the object with the plane on which it is sliding. All pushing forces will be restricted to lie in the plane. The results may be applied to three-dimensional objects, so long as the vertical component of the pushing force is negligible, and so long as the point of contact is near the table.

In the general case, when an object is being pushed there is only one point of contact between the object and the pusher. The contact may be where the front edge of a pushing fence touches a corner of the object (figure 1-2), or it may be where a pushing point touches an edge of the object (figure 2-1). In most of this paper we will assume that the pusher is a point in contact with an edge of the object. The analysis applies equally well if the pusher is a fence in contact with a corner of the object. In many figures (e.g., figure 2-3) an 'edge' will be drawn, and it will be left ambiguous whether this is the pushed edge of the object or the front edge of a fence.

It is assumed the pusher will move along a predetermined path in the plane, i.e., it is under position control. The object retains two degrees of freedom, with the third degree of freedom of its motion fixed by the contact maintained between the pusher and the object.

These two degrees of freedom are most conveniently expressed as the coordinates of a point in the plane called the *center of rotation* (COR). Any infinitesimal motion of the object can be expressed as a rotation $\delta\theta$ about some COR, chosen so that the infinitesimal motion of each point $\vec{w}$ of the object is perpendicular to the vector from the COR to the point $\vec{w}$. If the object is a disk, and the motion it

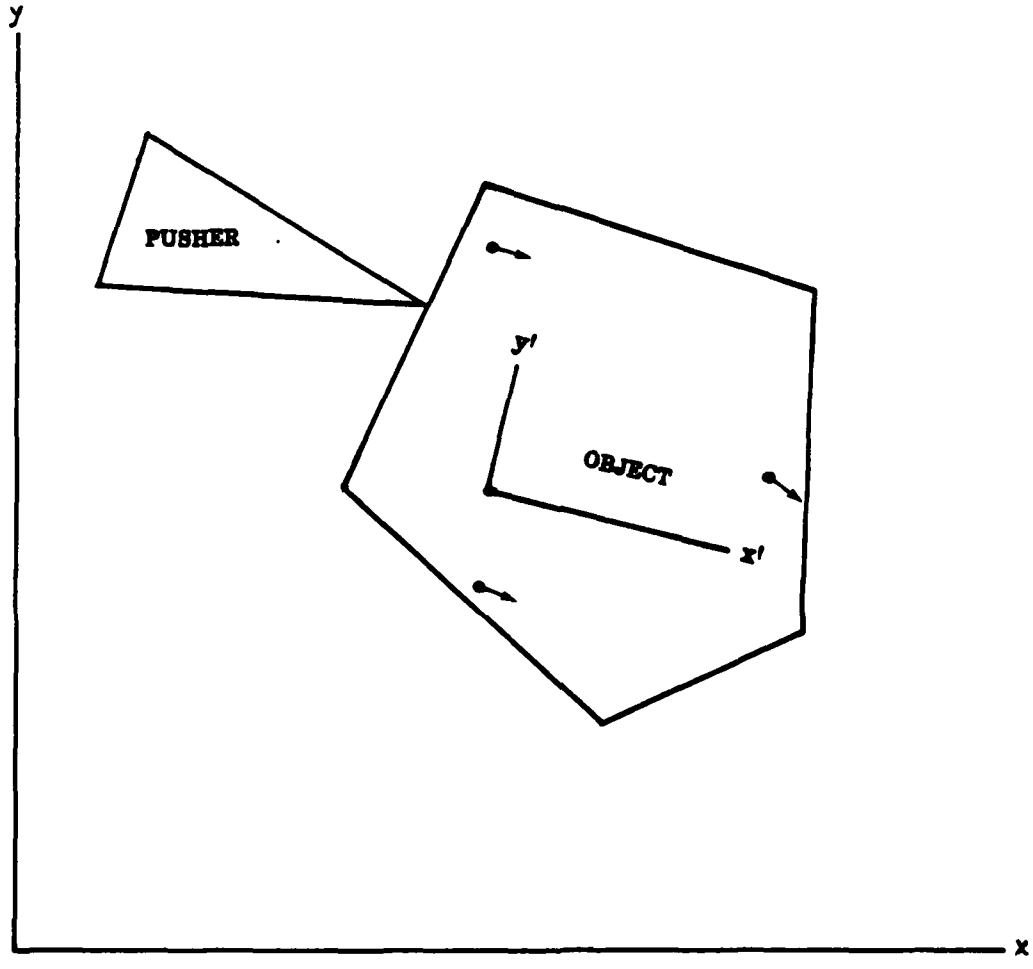

Figure 2-1: An object being pushed has two degrees of freedom

performs is pure rotation in place, the COR is at the center of the disk. Motions we might describe as "mostly translation" correspond to CORs far from the point of contact. In the extreme case, pure translation occurs when the COR is at infinity.

This paper is concerned with finding the COR.

2.2. The Support Distribution

Finding the COR is complicated by the fact that changes in the distribution of support forces under the object substantially affect the motion. Intuitively, if the support is concentrated near the center of mass (CM), the object will tend to rotate more and translate less than if the support is uniformly distributed over the entire bottom surface of the object. With support concentrated near the CM, much less energy is expended in rotating than with more dispersed support.

The distribution of support may be changed dramatically by tiny deviations from flatness of the bottom surface of the object (or of the surface it is sliding on). Indeed, if the object and the surface are sufficiently rigid and not perfectly flat, they may be expected to make contact at only three points. The three points may be located anywhere on the object's bottom surface, but like the legs of a three-legged stool, the triangle formed by the three points of support must enclose the projection of the CM onto the surface. Otherwise the object is unstable. This observation perhaps gives some intuitive justification to a theorem proved by Mason (Mason, 1985) which states that all extreme values of the location of the COR may be attained by considering only support distributions consisting of three points of support (a "tripod").

Since any assumption we could make about the form of the support distribution (for instance that it is uniform under the object as in (Prescott, 1923)) would not be justified in practice, our goal is to find the locus of CORs under *all* possible support distributions. Let the CM be at the origin, and $\vec{w}$ be a point in the plane. All that is known about the support distribution $S(\vec{w})$ is that

- $S(\vec{w})$ is zero outside the object,
- $S(\vec{w}) \geq 0$ everywhere,
- the total support force $\int S(\vec{w})\, d\vec{w} = Mg$, the weight of the object, and
- the first moment of the distribution, $\int S(\vec{w})\, \vec{w}\, d\vec{w} = 0$. (i.e., the centroid of the distribution is at the CM of the object, which is at the origin.)

2.3. Overview

The coefficient of friction with the supporting surface (μ_s) does not affect the motion of the object if we use a simple model of friction. We assume that μ_s is constant over space, that it is independent of normal force magnitude and tangential force magnitude and direction, and that it is velocity independent. In short, we assume Coulomb friction.

Initially we consider only $\mu_c = 0$, where μ_c is the friction coefficient between the edge of the object and the pusher. (In a subsequent paper we will do the analysis needed to treat $\mu_c > 0$.) We assume that the contact between the pusher and the object is restricted to a single point.

It is also assumed that all motions are slow. This *quasi-static approximation* requires that frictional forces on the object due to the coefficient of friction with the surface μ_s quickly damp out any kinetic energy of the object:

$$\frac{Mv^2}{2} \ll XMg\mu_s \tag{1}$$

where v is the velocity of the object and X is the precision with which it is desired to calculate distances.

In this paper we will assume the object being pushed is a disk with its CM at the center. Given another object of interest (e.g. a square), we can consider a disk centered at the CM of the square, big enough to enclose it. The radius a of the disk is the maximum distance from the CM of the square to any point on the square. Since any support distribution on the square could also be a support distribution on the disk, the COR locus of the disk must enclose the COR locus of the square. The locus for the disk provides useful bounds on the locus for the real object.

Other parameters of the problem are the point of contact $\vec{c}$ between the pusher and the object, and the angle α between the edge being pushed and the line of pushing, as shown in figure 2-2. The values of α and $\vec{c}$ shown are useful in considering the motion of the five-sided object shown inscribed in the disk. We do not require the point of contact to be on the perimeter of the disk, as this would eliminate applicability of the results to objects inscribed in the disk. Indeed, for generality we do not even require the point of contact to be within the disk. Similarly, we will not require α to be such that the edge being pushed is perpendicular to vector $\vec{c}$, as it would be if the object were truly a disk. The disk (with radius a), α, $\vec{c}$, and the CM, are shown in figure 2-2. A particularly simple distribution of support forces $S(\vec{w})$, in which the support is concentrated at just a "tripod" of points $(\vec{w}_1, \vec{w}_2, \vec{w}_3)$ is

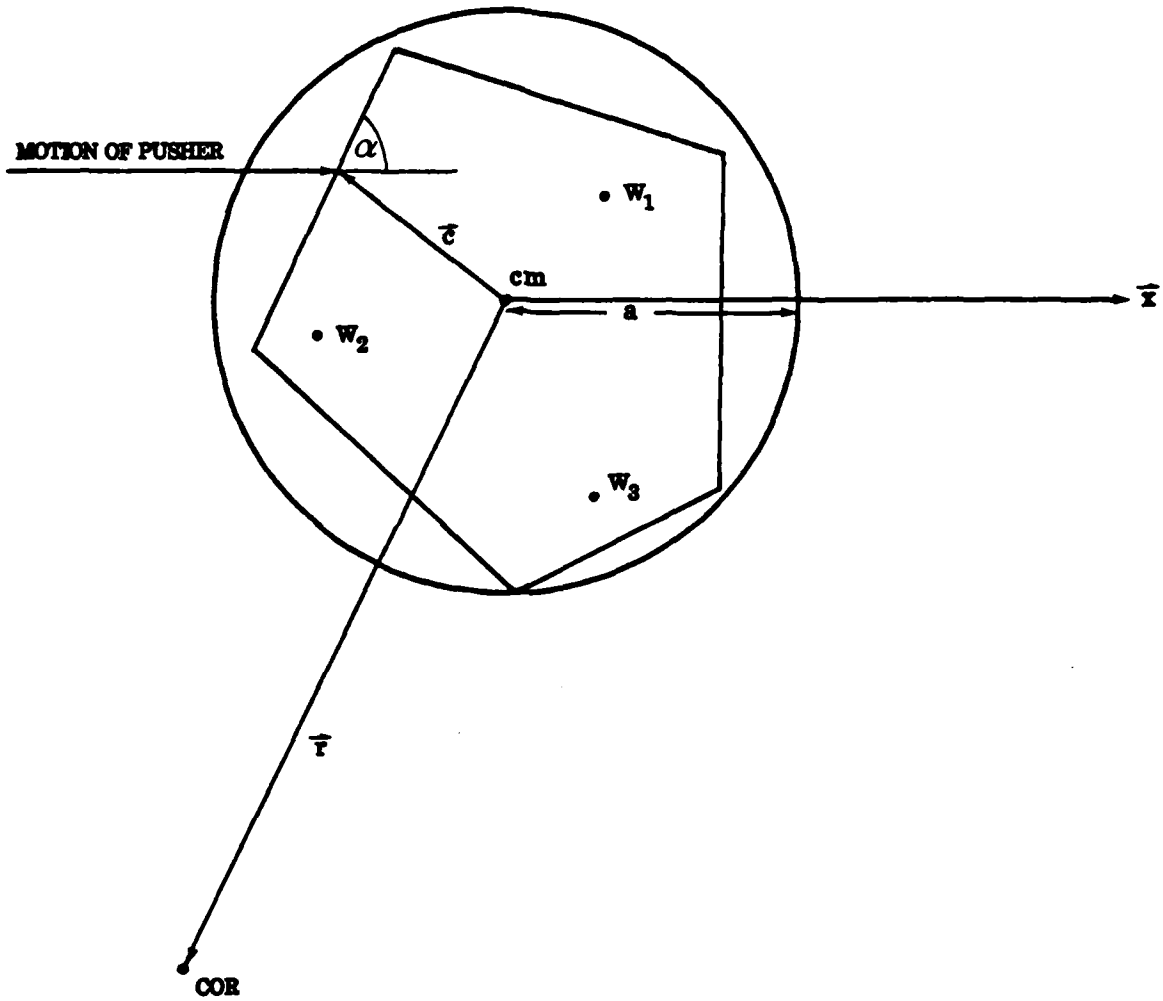

Figure 2-2: Parameters of the pushing problem

indicated, along with the COR for that distribution of support.

In section 3, we derive the energy E_r lost to friction when the pusher advances a distance δx. This is a function of the presumed location of the COR $\vec{r}$. The system will rotate about the COR which minimizes E_r, as proved in the appendix. We will find the COR by setting $\nabla E_r = 0$.

Using hundreds of thousands of randomly selected tripods satisfying the conditions listed in section 2.2, we can find the COR by numerically minimizing E_r for each tripod. Plotting the resulting CORs gives a rough idea of the COR locus, for a single choice of $\vec{c}$ and α (figure 2-3).

While Mason's theorem 5 states that *extremal* values (i.e., the boundary) of the COR locus may be found by considering only tripods of support, we see that in fact all values interior to the locus are attained in this way as well. The dense central region of the numerically generated locus in the figure has been replaced by hashing to facilitate printing.

In section 4, we express the equation $\nabla E_r = 0$ in terms of a new construction called the *quotient locus*. Each element of the quotient locus is a quotient of two moments of the support distribution S.

A surprising discovery is that all elements of the quotient locus for the disk may be attained by considering only *pairs* of points of support (dipods), instead of tripods. This statement therefore applies to the COR locus, as well. Using this information we calculate the analytic form of the boundaries of the quotient locus.

Once the quotient locus is found for a given object and pushing geometry, we calculate (in section 5) the boundaries of the COR locus from it. The greatest distance from any point in the COR locus to the CM, and its direction, are found analytically. These results, all that are needed for many applications, are of simple form and have a convenient graphical interpretation.

In section 6 we solve some sample problems using the results. One result is a simple formula for the maximum distance an object must be pushed by a fence to assure that it has rotated into alignment with the fence.

2.4. Notation

- Vectors are indicated by an arrow, e.g., $\vec{v}$.
- $\vec{r}$ is the vector from the CM to the COR. r is the magnitude of that vector, i.e., the

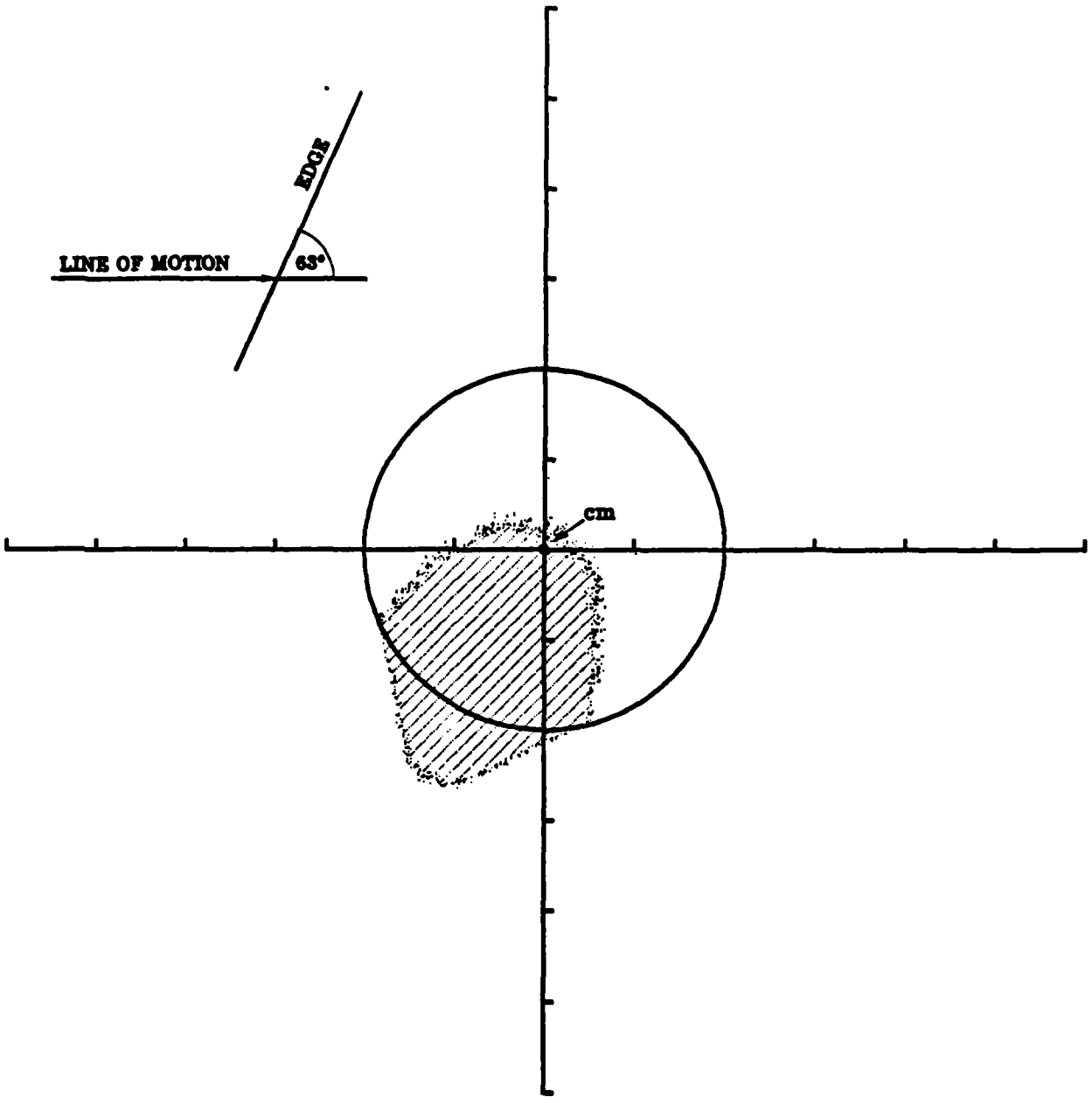

Figure 2-3: COR locus found by iterative minimization (dots)

distance from the CM to the COR.

- A Greek letter is used to represent both an *angle* and a *unit vector* which makes that angle with respect to the x-axis (measured CCW). An arrow is used to indicate the unit vector: $\vec{\alpha} = (\cos\alpha, \sin\alpha)$.
- We indicate functional dependence with subscripts. E_r is a function of $\vec{r}$ (the COR).
- All integrals are over the area of the disk.
- Curly brackets indicate a locus of values of a quantity.

3. Minimizing the Energy

In this section we compute the energy that is dissipated due to friction when the pusher advances a distance δx, for a given center of rotation $\vec{r}$, and for a given distribution of support $S(\vec{w})$. (figure 2-2).

It may help to imagine the disk "pinned" at the COR. This is not difficult to imagine if the COR happens to fall inside the perimeter of the disk, and one's intuition can be extended to include the case where the COR is outside the perimeter. Either way, the disk is free to rotate *only about the COR*, and the COR itself stays stationary.

Given the COR, the motion of the disk is fully determined when we apply one more constraint: the edge being pushed (at $\vec{c}$) must move out of the way of the advancing pusher, but stay in contact.

3.1. Relation between Motion of Pusher and Rotation of Object

In order to accommodate the advance δx of the pusher, the disk will rotate an amount $\delta\theta$ about the center of rotation $\vec{r}$. A rotation of $\delta\theta$ allows an advance of the pusher δx consisting of two parts, as shown in figure 3-1.

$$\delta x_1 = \delta\theta\,|\vec{c} - \vec{r}|\cos\theta = \delta\theta\,(c_y - r_y) \tag{2}$$

$$\delta x_2 = \delta x_1 \frac{\tan\theta}{\tan\alpha} = \delta\theta \frac{c_x - r_x}{\tan\alpha}$$

$$\delta x = \delta x_1 + \delta x_2 = \delta\theta\,(c_y - r_y + \frac{c_x - r_x}{\tan\alpha})$$

Note that δx_2 corresponds to slipping of the point of contact along the object edge.

Defining the unit vector $\vec{\alpha} = (\cos\alpha, \sin\alpha)$ we can write

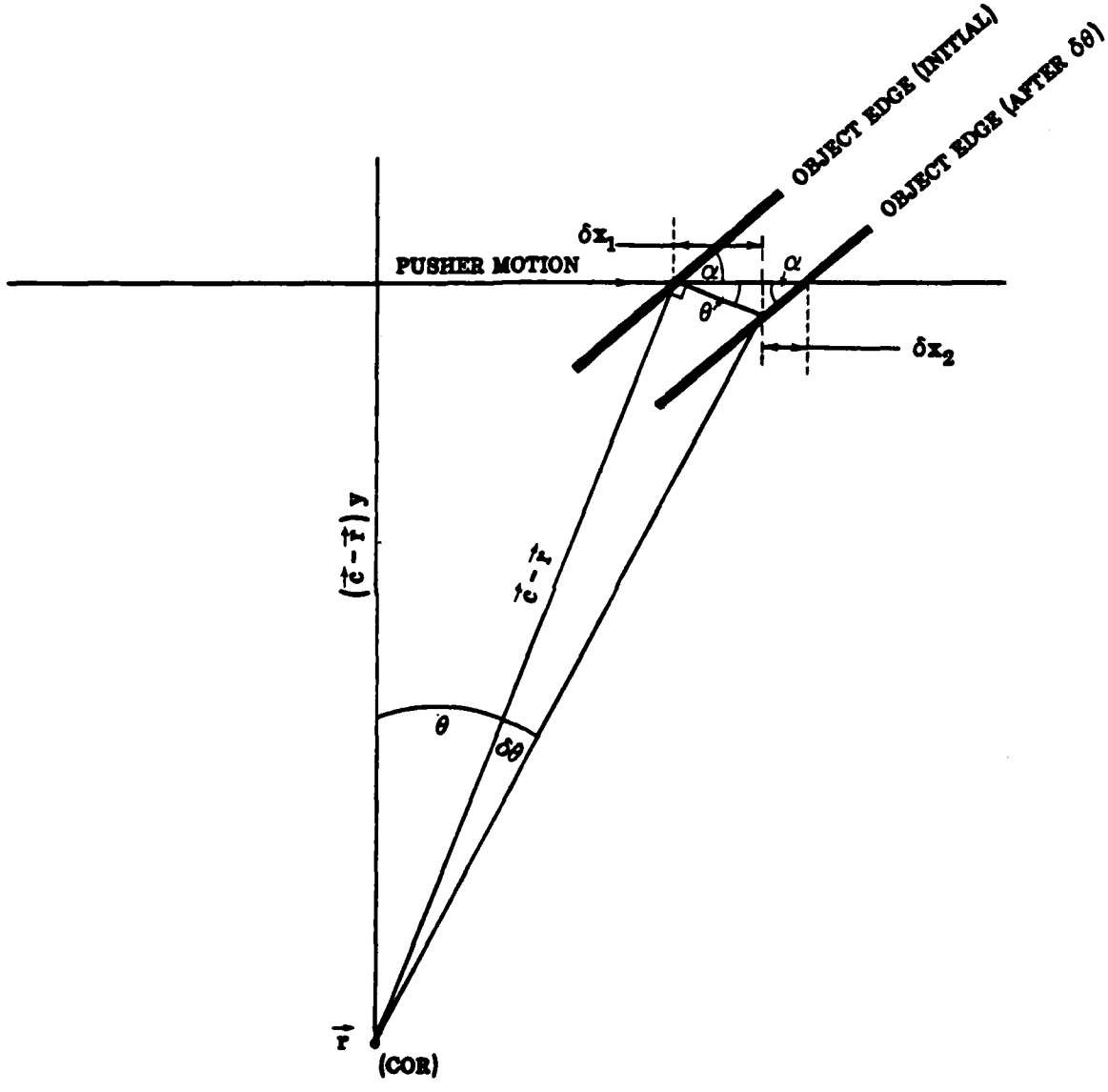

Figure 3-1: Relation between advance of pusher (δx) and rotation about the COR ($\delta\theta$)

$$\delta x = \frac{\delta\theta}{\sin\alpha}\,\vec{\alpha}\cdot(\vec{c}-\vec{r})\,. \tag{3}$$

To avoid proliferation of absolute value signs, henceforth $\vec{\alpha}\cdot(\vec{c}-\vec{r})$ will be taken to be positive. Considerations of symmetry will allow application of the results to cases where $\vec{\alpha}\cdot(\vec{c}-\vec{r})$ is negative. Physically, $\vec{\alpha}\cdot(\vec{c}-\vec{r})>0$ corresponds to clockwise rotation of the object as it is pushed.

3.2. Energy Lost to Friction with the Table

An element of the disk at $\vec{w}$ supports a force $S(\vec{w})\,d\vec{w}$ normal to the table. The element will slide a distance

$$\delta\theta\,|\vec{w}-\vec{r}\,| \tag{4}$$

due to the rotation $\delta\theta$ about the center of rotation $\vec{r}$, and in the process will dissipate an amount of energy

$$dE_r = \mu_s\,S(\vec{w})\,d\vec{w}\,\delta\theta\,|\vec{w}-\vec{r}\,|\,. \tag{5}$$

Integrating over the area of the disk, the total energy dissipated due to rotation $\delta\theta$ is

$$E_r = \delta\theta\,\mu_s\int S(\vec{w})\,|\vec{w}-\vec{r}\,|\,d\vec{w} \tag{6}$$

where we write E_r to remind ourselves that the energy is a function of the presumed location of the center of rotation $\vec{r}$. Substituting for $\delta\theta$, we have

$$E_r = \frac{\delta x\,\mu_s\sin\alpha}{\vec{\alpha}\cdot(\vec{c}-\vec{r})}\int S(\vec{w})\,|\vec{w}-\vec{r}\,|\,d\vec{w}\,. \tag{7}$$

The system will find a location for $\vec{r}$ which minimizes E_r. At this minimum the derivatives of E_r with respect to both $\vec{r}_x$ and $\vec{r}_y$ must be zero. Evaluating the derivative of E_r with respect to $\vec{r}$ and setting it equal to zero we find

$$\nabla E_r = \delta x\,\mu_s\sin\alpha\,\frac{[d_r\,\vec{\alpha}-\vec{v}_r\,\vec{\alpha}\cdot(\vec{c}-\vec{r})]}{[\vec{\alpha}\cdot(\vec{c}-\vec{r})]^2} = 0 \tag{8}$$

where

$$d_r = \int S(\vec{w}) \, | \vec{w} - \vec{r} \, | \, d\vec{w} \tag{9}$$

a scalar, can be physically interpreted as the weighted *distance* from the COR to the support distribution, and

$$\vec{v}_r = \int S(\vec{w}) \frac{\vec{w} - \vec{r}}{| \vec{w} - \vec{r} |} d\vec{w} \tag{10}$$

a vector, can be interpreted as the weighted *direction* from the COR to the support distribution.

Equation 8 expresses the physical principle that the system will execute that instantaneous motion which minimizes energy. Energy is not always minimized in dissipative systems. However it is possible to show that Newton's laws require the numerator of equation 8 to be zero at the correct COR (see Appendix.) The energetic derivation above is simpler.

3.3. Iterative Numerical Solution

Minimization of E_r can be carried out in an iterative manner to find the COR for a given support distribution $S(\vec{w})$. Figure 2-3 shows the locus of CORs obtained in this manner. Each point is the COR for a randomly chosen three-point support distribution. Only support distributions consisting of three points (a tripod) need be considered since according to Mason's theorem 5 three points are sufficient. Weights were computed for the three points in such a way as to satisfy the constraint that the CM be at the center of the disk. (If this required any of the weights to be negative, the tripod was discarded.) An initial guess was made for the location of the center of rotation $\vec{r}$, and ∇E_r evaluated at that point.

The minimization technique used requires computation of $\nabla(\nabla E_r)$, the second derivative of E_r, a two-by-two matrix, which can be obtained analytically. A new guess for $\vec{r}$ is then made by adding to the old guess

$$\Delta \vec{r} = \frac{-\nabla E_r}{\nabla(\nabla E_r)}. \tag{11}$$

This method usually converged quickly if the initial guess was sufficiently close to the correct answer. By moving only one leg of the tripod at a time, and by only a small amount, the value of $\vec{r}$ found for

one tripod could be used as an initial guess for the next. Figure 2-3 represents 590000 tripods, taking 4 CPU hours on a VAX-780. Similar figures, done with four points of support instead of tripods, are identical.

Numerical methods may converge to a local rather than a global minimum, if more than one minimum exists. Here $\nabla E_r = 0$ if and only if Newton's laws are satisfied for a given value of the COR, i.e., if the forces balance. Distinct locations of the COR correspond one-to-one with distinct motions of the pushed object. There can be only one motion of the object satisfying Newton's laws, so there can be only one minimum of E_r.

4. The Quotient Locus

Resuming our analytical discussion from section 3.2, we set $\nabla E_r = 0$ in equation 8. The constant terms drop out leaving

$$r^2 \vec{\alpha} = \vec{q}_r [\, \vec{\alpha} \cdot (\vec{c} - \vec{r})] \tag{12}$$

where we define the *quotient moment*, a vector, as

$$\vec{q}_r = r^2 \frac{\vec{v}_r}{d_r}. \tag{13}$$

It is a function of $\vec{r}$ and the distribution $S(\vec{w})$, and has units of distance. In this section we *hold the center of rotation $\vec{r}$ fixed*, and analyze the quotient moment for all support distributions $S(\vec{w})$.

The *quotient locus* $\{\vec{q}_r\}$ is the set of $\vec{q}_r$ for all possible choices of the distribution S consistent with the requirements listed in section 2.2. It is still a function of $\vec{r}$, but the dependence on S has been removed.

We will always plot the quotient locus displaced by $\vec{r}$, i.e., based at the COR. $\{\vec{q}_r\}$ may be plotted as a region of space, if we remember that a given $\vec{q} \in \{\vec{q}_r\}$ is a *vector* with its tail at the COR and its head anywhere in that region.

We will find the boundary of the quotient locus. The results will allow us to find the boundary of the COR locus in section 5.

To simplify discussion, we take the total weight of the object $Mg = 1$, that is

$$Mg = \int S(\vec{w})\, d\vec{w} = 1 . \tag{14}$$

Since multiplying the support distribution S by a constant factor changes both numerator and denominator of $\vec{q}_r$ by that same factor, the assumption is harmless. Physically, the mass of the disk has no effect on the motion, so we can choose it arbitrarily.

4.1. Extrema of the Quotient Locus

Since $\vec{v}_r$ (equation 10) can be interpreted as a weighted average of *unit vectors* from the COR to the support distribution, the greatest magnitude $\vec{v}_r$ can have will be 1, and will be attained when the support distribution is concentrated at the CM. In all other cases the direction to elements of the support distribution varies, and so some cancellation is inevitable. When the magnitude of $\vec{v}_r$ is maximal, it must be directed from the COR to the CM.

The smallest magnitude $\vec{v}_r$ can achieve depends on whether the COR is inside or outside the disk, i.e., on whether $r > a$ or $r < a$, where a is the radius of the disk. In either case we wish to achieve the maximum amount of cancellation of direction possible. If $r > a$ this occurs when the support distribution consists of two points at opposite edges of the disk, providing the minimum possible agreement on direction between the two vectors, as shown in figure 4-1.

If $r < a$, we can arrange for $\vec{v}_r$ to be zero. Indeed we can arrange for $\vec{v}_r$ to point from the COR maximally *away* from the CM by making a two-point support distribution as shown in figure 4-2. (In the figure the distance from w_2 to the COR is infinitesimal.) The two vectors $\vec{w}_1$ and $\vec{w}_2$ point in opposite directions. To maintain the centroid of the support distribution at the CM, we find the weights of $\vec{w}_1$ and $\vec{w}_2$ are

$$S_1 = \frac{r}{r+a}, \text{ and} \tag{15}$$
$$S_2 = \frac{a}{r+a}.$$

Therefore $\vec{w}_2$ is more heavily weighted than $\vec{w}_1$, and

$$\vec{v}_r = S_1\vec{v}_1 + S_2\vec{v}_2 = (S_2 - S_1)\vec{v}_2 = \frac{a-r}{a+r}\vec{v}_2 \tag{16}$$

points from the COR *away* from CM.

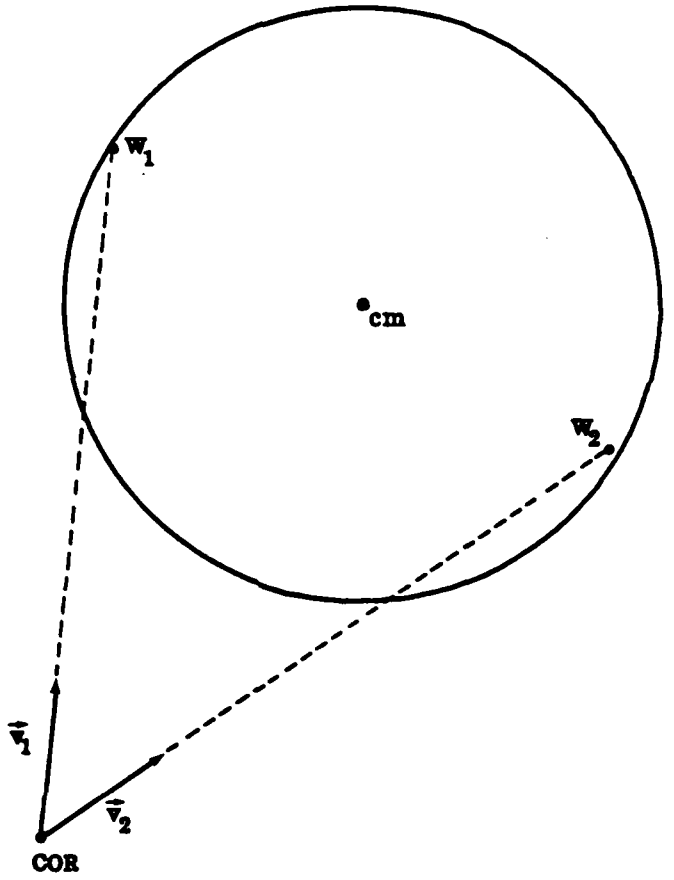

Figure 4-1: Dipod responsible for the smallest value of $\vec{v}_r$, for $r > a$

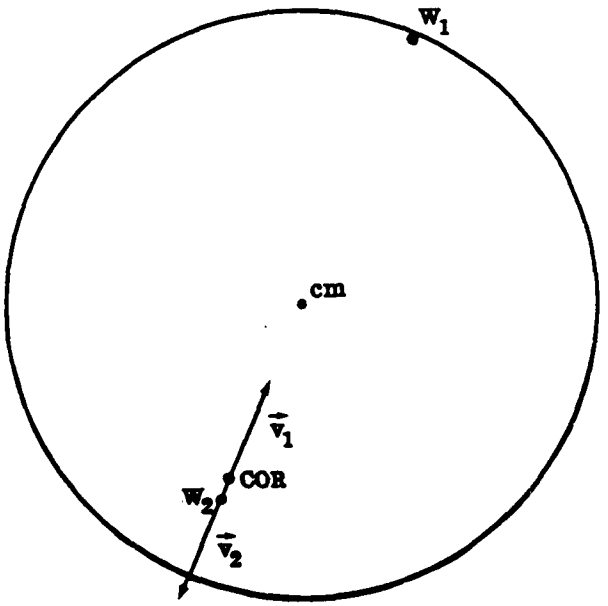

Figure 4-2: Dipod responsible for a negative value of $\vec{v}_r$, for $r < a$

Now consider d_r (equation 9). Clearly if the support distribution is concentrated at the CM, the weighted distance from the COR to the support distribution is just r. In fact r is the smallest value which d_r can attain. In the configuration shown in figure 4-2,

$$d_r = S_1 \cdot (a + r) + S_2 \cdot 0 = r . \tag{17}$$

d_r takes on its maximum value when the support distribution consists of two points as in figure 4-1. That value is

$$d_r = (r^2 + a^2)^{1/2} . \tag{18}$$

Since $\vec{q}_r$ is the quotient of $\vec{v}_r$ and d_r, extreme values of $|\vec{q}_r|$ occur when $\vec{v}_r$ is maximal and d_r minimal, and when $\vec{v}_r$ is minimal and d_r maximal.

4.2. Numerical Solution for the Quotient Locus

Having found the extreme values of $\vec{q}_r$ above, we can find the locus of all possible quotients numerically. It is much easier to find the $\{\vec{q}_r\}$ locus (for a given value of $\vec{r}$) than it is to find the COR locus. No iteration is required; for a given tripod, $\vec{v}_r$ and d_r can be calculated immediately. Figures 4-3 and 4-4 show typical $\{\vec{q}_r\}$ loci for $r<a$ and $r>a$, respectively. The dots are values of $\vec{q}_r$ found numerically, while the solid curve is the empirical boundary of the locus as described below.

The dots in figures 4-3 and 4-4 represent over 3,000,000 and 500,000 randomly chosen tripods, respectively. The solid curves which appear to bound the dots are generated by two classes of dipods, discussed below. Since dipods are a special case of tripods, the solid curve is in $\{\vec{q}_r\}$. On the basis of numerical studies such as shown in these figures, we believe that no value of $\vec{q}_r$ generated by a tripod falls outside the dipod curve. Therefore the dipod curve is the exact boundary of $\{\vec{q}_r\}$. We have not been able to prove analytically that no tripod value of $\vec{q}_r$ falls outside the dipod curve, so the boundaries should be considered empirically justified only.

4.3. Boundary for |COR| < a

We observe that for $r<a$ the boundary of the locus is a circle. This empirical boundary can be generated by two-point support distributions (dipods) of the type shown in figure 4-5, where the angle ω can vary. These dipods are a generalization of the one shown in figure 4-2. (The distance from $\vec{r}$ to $\vec{w}_2$ is infinitesimal.) We can then calculate a parametric form for the boundary in terms of ω:

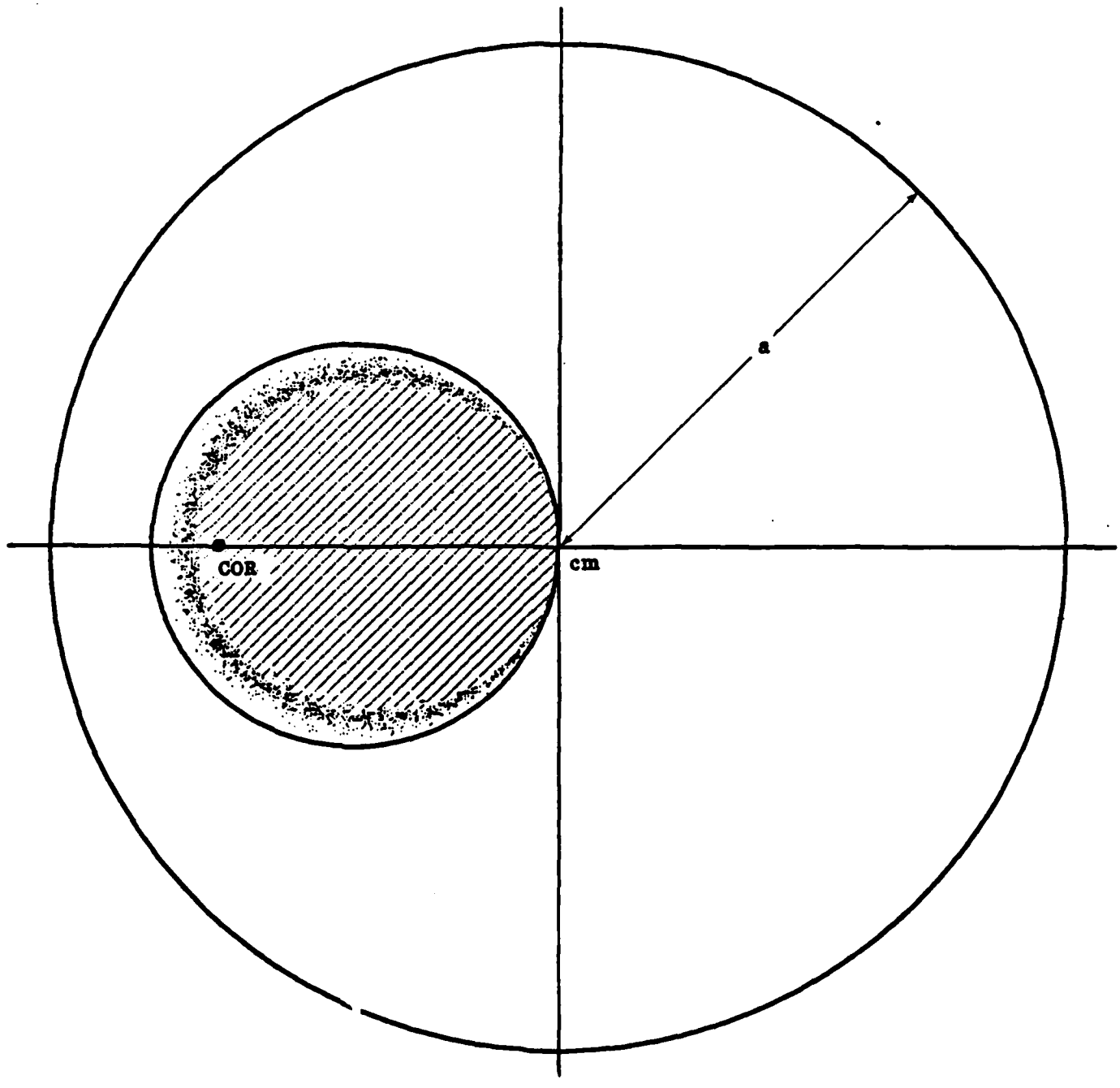

Figure 4-3: Quotient locus $\{\vec{q}_r\}$ (dots), and empirical boundary (solid), for $r < a$

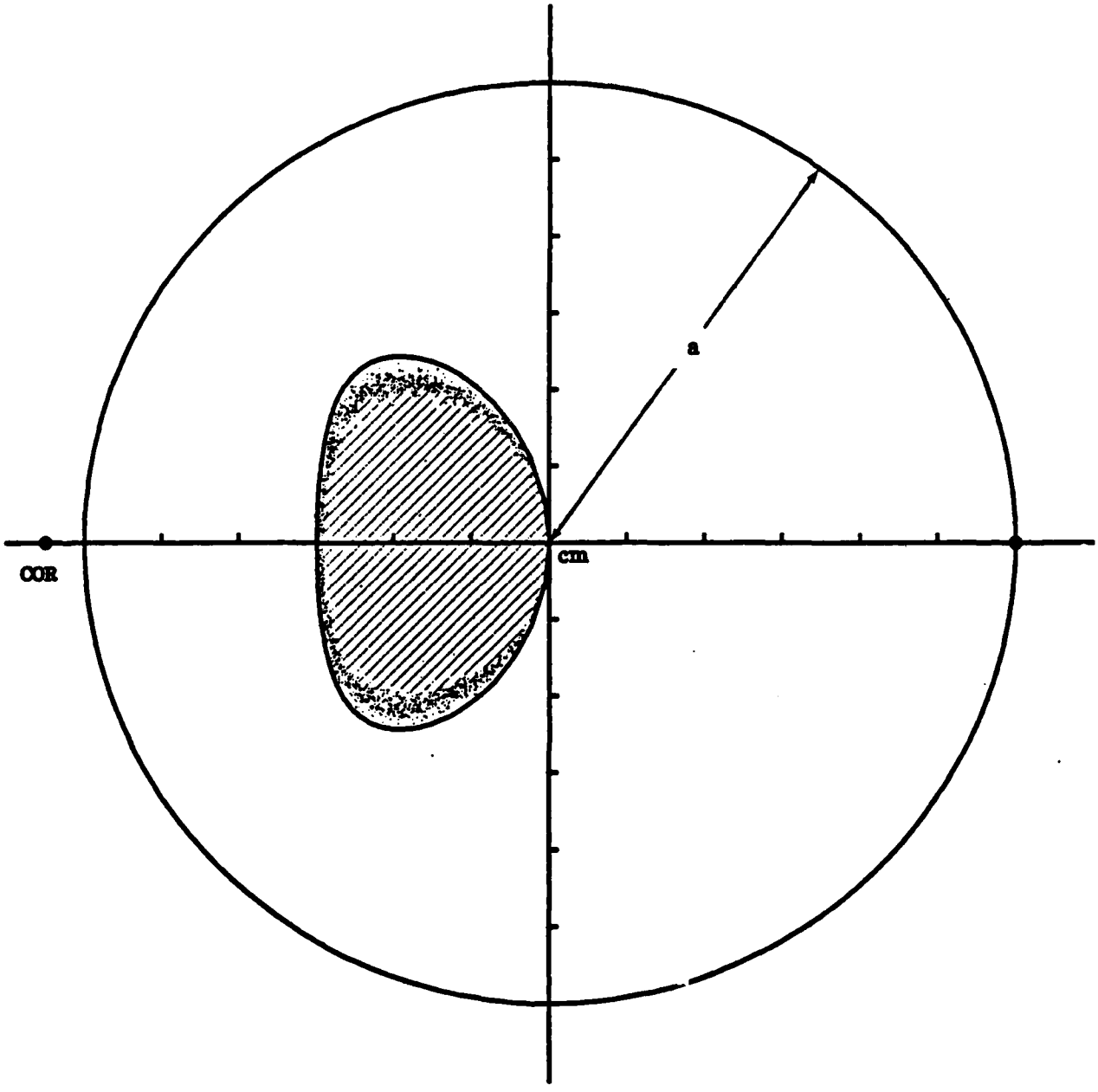

Figure 4-4: Quotient locus $\{\vec{q}_r\}$ (dots), and empirical boundary (solid), for $r > a$

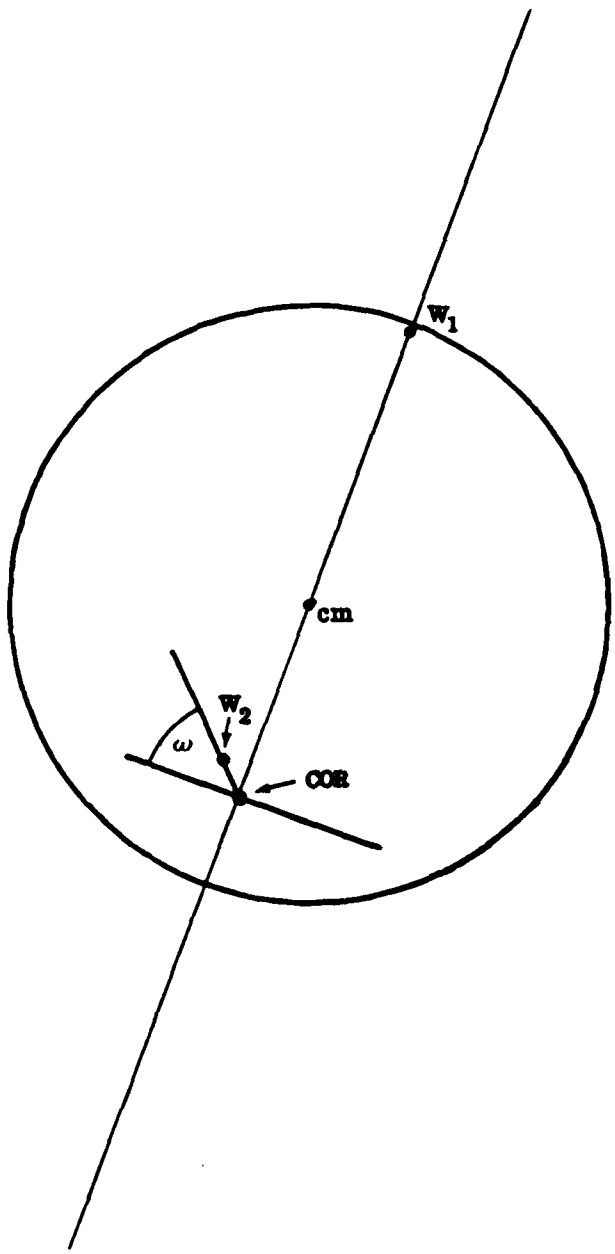

Figure 4-5: Dipods contributing to the boundary of $\{\vec{q}_r\}$, for $r<a$

$$\vec{q}_r = \vec{\omega}\frac{r}{r+a}(a\vec{\omega} - \vec{r}) \tag{19}$$

where $\vec{\omega} = (\cos\omega, \sin\omega)$

This generates a circle of radius

$$b = \frac{a\,r}{r+a}. \tag{20}$$

4.4. Boundary for |COR| > a

For $r > a$, the empirical boundary of the locus $\{\vec{q}_r\}$ is generated by dipods of the type shown in figure 4-6, where ω is allowed to vary. These dipods are a generalization of the dipod shown in figure 4-1. Again, the boundary can be calculated parametrically from ω (via intermediate terms d^+, d^-, γ^+, and γ^-) as

$$d^{\pm} = (r^2 + a^2 \pm 2a\,r\cos\omega)^{1/2} \tag{21}$$

$$\sin\gamma^{\pm} = \frac{a\sin\omega}{d^{\pm}}$$

$$\cos\gamma^{\pm} = (1 - \sin^2\gamma^{\pm})^{1/2}$$

$$\vec{v}_r = \left(\frac{\cos\gamma^+ + \cos\gamma^-}{2}, \frac{\sin\gamma^+ - \sin\gamma^-}{2}\right)$$

$$d_r = \frac{d^+ + d^-}{2}$$

$$\vec{q}_r = r^2\frac{\vec{v}_r}{d_r}.$$

It is the boundaries of $\{\vec{q}_r\}$ that will be used (in section 5) to determine the boundaries of the COR locus. Therefore the boundaries of the COR locus, too, can be found by considering only dipods. This is a stronger statement than Mason's theorem 5, which requires tripods. Additionally, we have found the two points constituting the dipods. However, it should be noted that the sufficiency of tripods holds for any object, whereas dipods are sufficient only for a disk.

Figures 4-3 and 4-4 demonstrate that the two classes of dipods considered above, and illustrated in figures 4-5 and 4-6, generate extremal quotient moments. In other words, the locus $\{\vec{q}_r\}$ of values of $\vec{q}_r$ for all distributions of support $S(\vec{w})$ satisfying the conditions of section 2.2 fall inside the empirical boundary generated by the above dipods. The boundaries themselves are, of course, part of $\{\vec{q}_r\}$

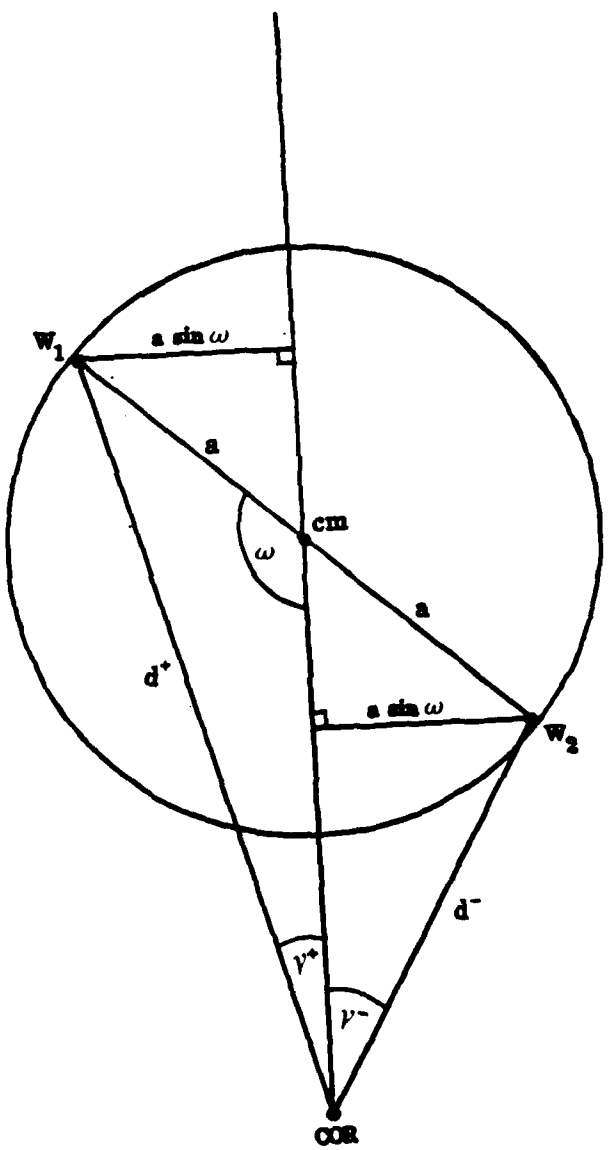

Figure 4-6: Dipods contributing to the boundary of $\{\vec{q}_r\}$, for $r > a$

since the boundaries are generated by acceptable distributions of support.

5. The COR Locus

Having found a parametric representation of the $\{\vec{q}_r\}$ locus, we can find the COR locus. Recall the requirement for minimizing the energy lost to friction (equation 12):

$$r^2\vec{\alpha} = \vec{q}_r\ [\vec{\alpha}\cdot(\vec{c}-\vec{r})]\,. \tag{22}$$

The COR locus is the set of all $\vec{r}$ for which there exists a $\vec{q}_r \in \{\vec{q}_r\}$ satisfying equation 22.

Equation 22 is a vector equation. The left side obtains its direction from $\vec{\alpha}$. The right side obtains its direction from $\vec{q}_r$, since $\vec{\alpha}\cdot(\vec{c}-\vec{r})$ is a scalar. To satisfy the vector equation $\vec{q}_r$ must have direction $\vec{\alpha}$. We can rewrite equation 22 in scalar form, retaining the direction constraint on $\vec{q}_r$ separately:

$$r^2 = |\vec{q}_r|\ [\vec{\alpha}\cdot(\vec{c}-\vec{r})] \tag{23}$$

where $\vec{q}_r \in \{\vec{q}_r\}$

and $\vec{q}_r \parallel \vec{\alpha}$

We wish to find the locus of $\vec{r}$ for all distributions $S(\vec{w})$. It is best to imagine $\vec{r}$ to be an independent variable. Each value of $\vec{r}$ yields a locus $\{\vec{q}_r\}$, with one element $\vec{q}_r \in \{\vec{q}_r\}$ corresponding to each distribution $S(\vec{w})$. For some values of $\vec{r}$ the value of $\vec{q}_r$ required to satisfy equation 23 is in $\{\vec{q}_r\}$; for other values it is not. The former values constitute the COR locus.

It is confusing, but unavoidable, that the locus $\{\vec{q}_r\}$ shifts as we consider different locations of the center of rotation $\vec{r}$. In figure 5-1 we have plotted several $\{\vec{q}_r\}$ loci for different values of $\vec{r}$. Note that varying the *magnitude* of $\vec{r}$ continuously changes the shape or size of the $\{\vec{q}_r\}$ loci. But changing the *direction* of $\vec{r}$ only causes a corresponding rotation of the $\{\vec{q}_r\}$ locus.

The variables of equation 23 are shown geometrically in figures 5-2, 5-3, and 5-4. In each figure we have plotted a value of $\vec{r}$ and the locus $\{\vec{q}_r\}$ for that $\vec{r}$. We then calculate and plot the value of $\vec{q}_r$ required to satisfy equation 23. In figure 5-2, the value of $\vec{q}_r$ required does not fall in $\{\vec{q}_r\}$, so the value of $\vec{r}$ shown is not in the COR locus. In figure 5-3, the value of $\vec{q}_r$ required *does* fall in $\{\vec{q}_r\}$, so the value of $\vec{r}$ shown is in the COR locus.

In figure 5-4, the value of $\vec{q}_r$ required to satisfy equation 23 happens to be on the boundary of the

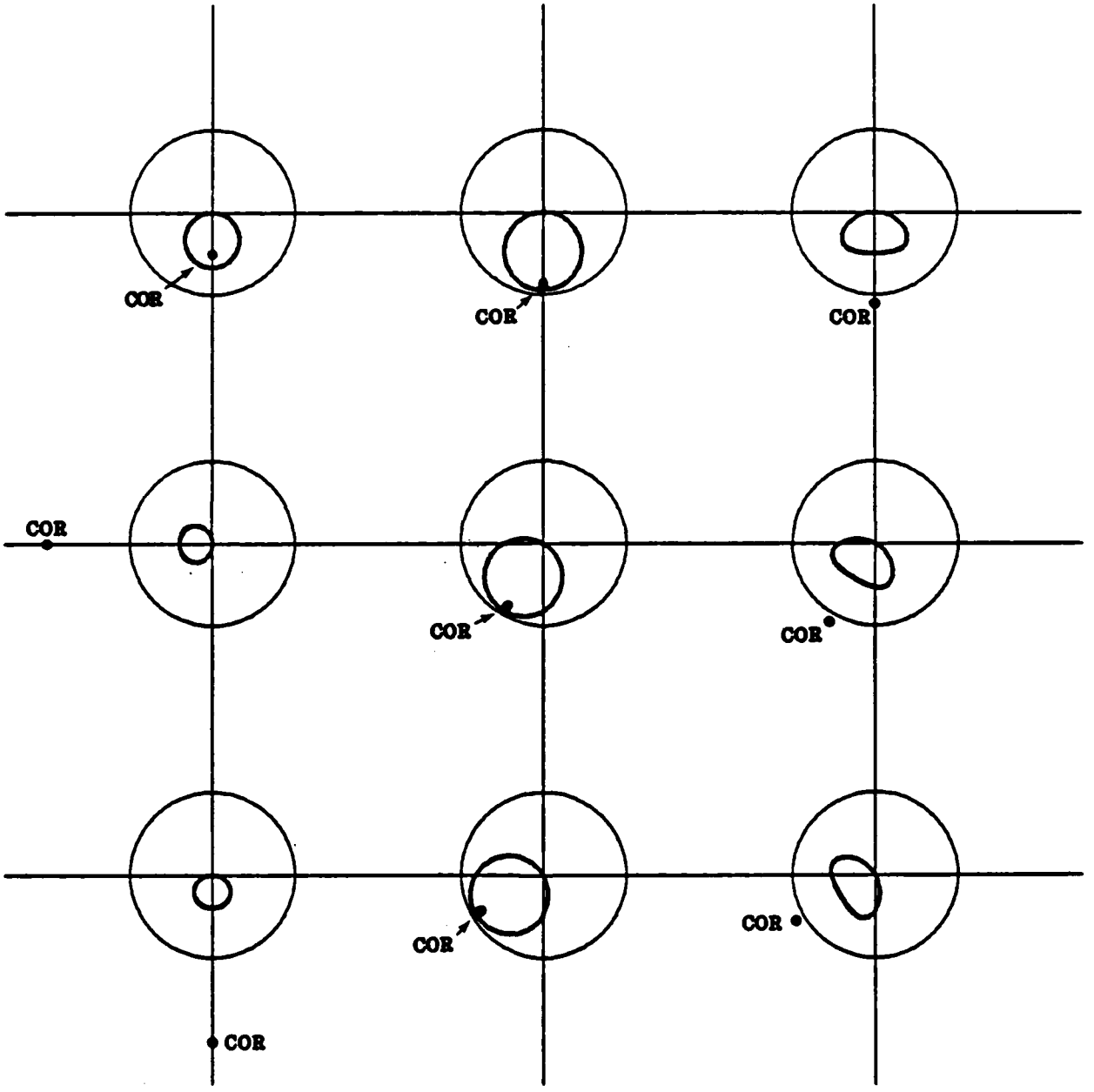

Figure 5-1: Boundaries of quotient loci $\{\vec{q}_r\}$ for various $\vec{r}$

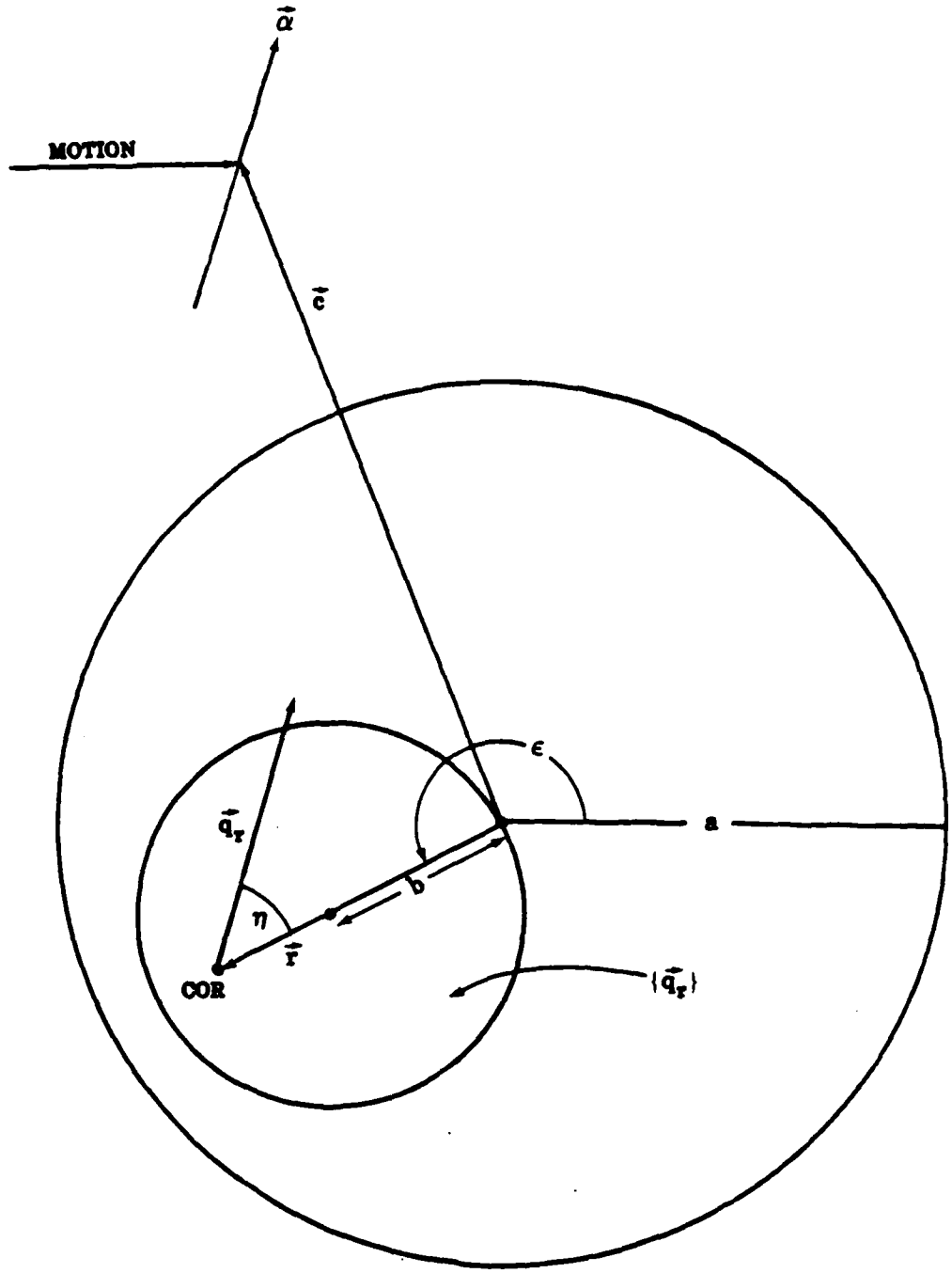

Figure 5-2: Variables of equation 23, for a value of $\vec{r}$ not in the COR locus

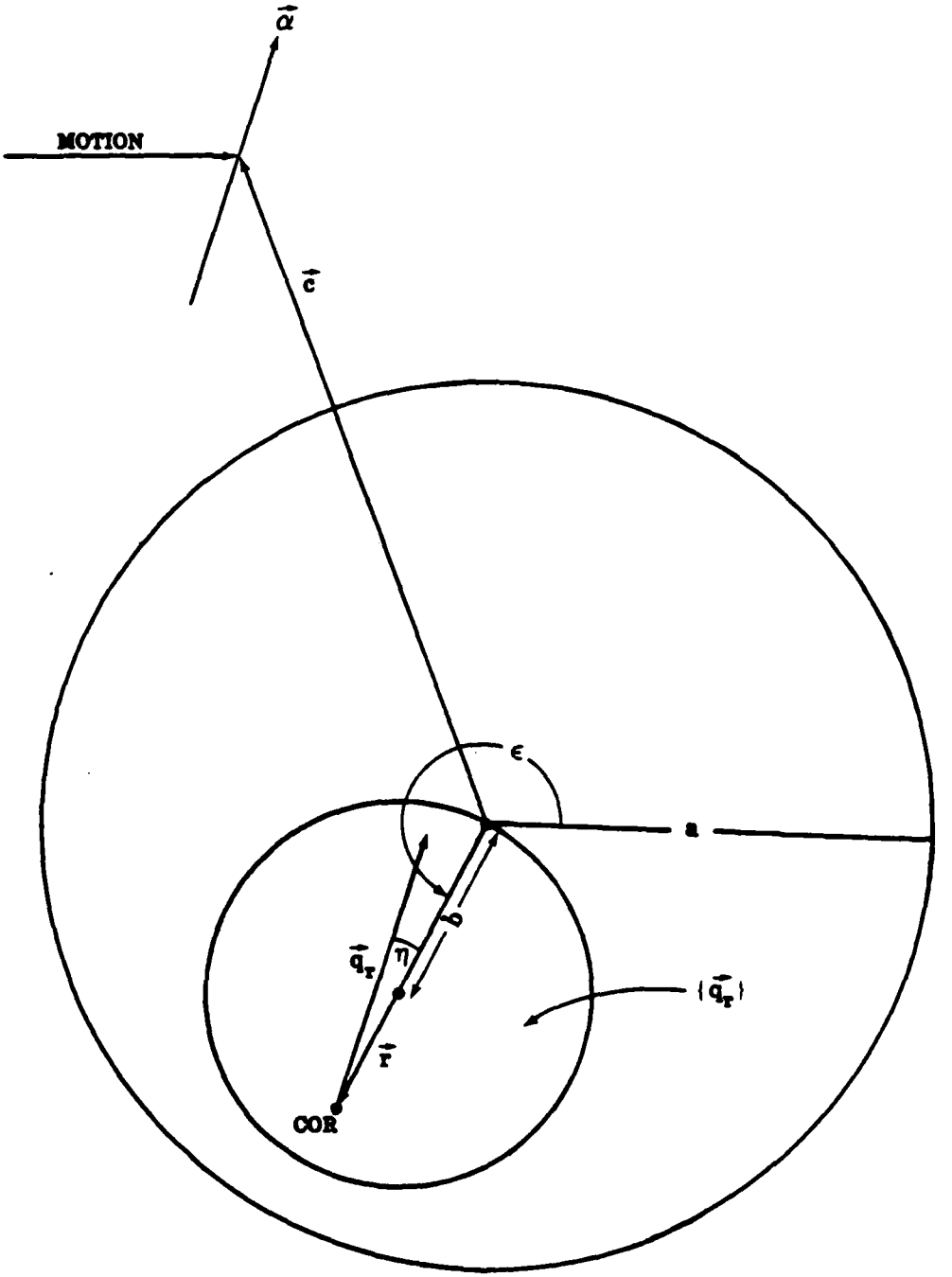

Figure 5-3: Variables of equation 23, for a value of $\vec{r}$ in the COR locus

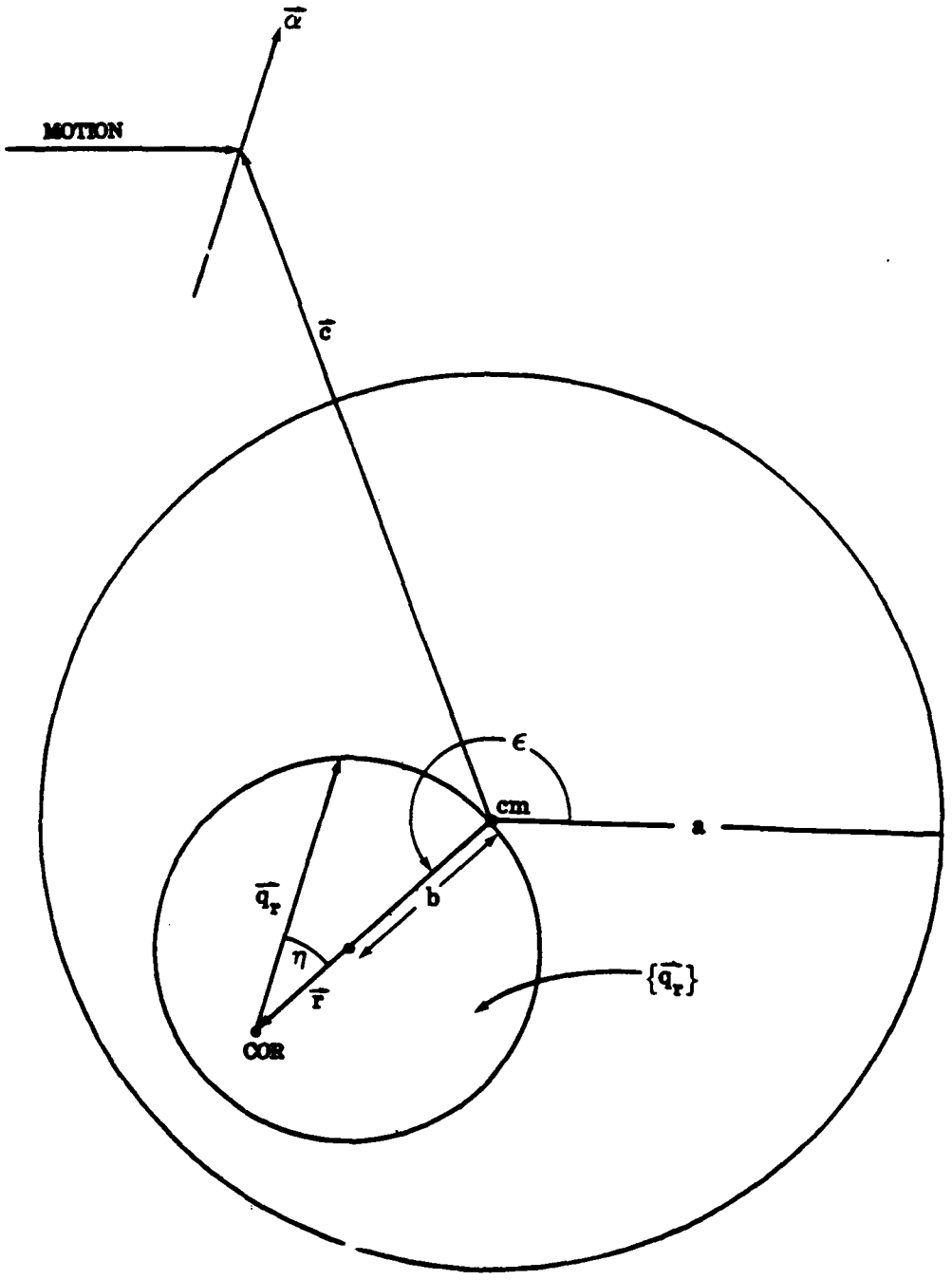

Figure 5-4: Variables of equation 23, for a value of $\vec{r}$ on the boundary of the COR locus

$\{\vec{q}_r\}$ locus. The boundary of the COR locus is generated by such cases. Interior points of the COR locus are generated when the $\vec{q}_r$ required is interior to the $\{\vec{q}_r\}$ locus, as in figure 5-3. Since we are interested only in the boundary of the COR locus, we will consider only values of $\vec{q}_r$ which are on the boundary of the $\{\vec{q}_r\}$ locus, as shown.

5.1. |COR| < a

It will be convenient to represent the COR by its polar coordinates (r, ε), and to define the relative angle η. Both angles are shown in figure 5-4. We have

$$\varepsilon = \pi + \alpha - \eta \,. \tag{24}$$

If $r < a$, the boundary of $\{\vec{q}_r\}$ is a circle. The condition that $\vec{q}_r$ lie on the circle can be expressed

$$\left| \, |\vec{q}_r| \; \vec{a} + (r-b)\vec{\varepsilon} \right| = b \,. \tag{25}$$

where b is the radius of the circle, from equation 20. Equation 25 can be expressed in terms of the angle η as

$$(|\vec{q}_r| - (r-b)\cos\eta)^2 + ((r-b)\sin\eta)^2 = b^2 \,. \tag{26}$$

Solving this quadratic equation for $|\vec{q}_r|$ we find

$$|\vec{q}_r| = (r-b)\cos\eta \pm (b^2 - ((r-b)\sin\eta)^2)^{1/2} \,. \tag{27}$$

Inserting this value of $|\vec{q}_r|$ into equation 23 and eliminating the square root we obtain

$$\left(\frac{r^2}{\vec{a}\cdot(\vec{c}-\vec{r})} - (r-b)\cos\eta\right)^2 = b^2 - ((r-b)\sin\eta)^2 \,. \tag{28}$$

Substituting b from equation 20 and simplifying we find

$$r^2(a+r) + (r-a)[\vec{a}\cdot(\vec{c}-\vec{r})]^2 - 2r^2[\vec{a}\cdot(\vec{c}-\vec{r})]\cos\eta = 0 \tag{29}$$

where $[\vec{a}\cdot(\vec{c}-\vec{r})] = \vec{a}\cdot\vec{c} + r\cos\eta$.

Equation 29 is a cubic in r and quadratic in $\cos\eta$. The solution for $\cos\eta$ is

$$\cos\eta = \frac{r((r+a)^2 + (\vec{\alpha}\cdot\vec{c})^2)^{1/2} - a(\vec{\alpha}\cdot\vec{c})}{r(r+a)}. \tag{30}$$

The other quadratic root is invalid. Since η is related by equation 24 to the polar angle ε, equation 30 describes the boundary of the COR locus in the polar coordinates r, ε, for $r < a$. A typical COR locus generated using equation 30 is shown in figure 5-5.

5.1.1. Extremal Radius of the COR Locus Boundary for |COR|<a

The minimum radius of the COR locus boundary occurs at $\varepsilon = \alpha$, which corresponds to $\eta = \pi$. From equation 29 we find

$$r_{min} = \frac{a(\vec{\alpha}\cdot\vec{c})}{2a + (\vec{\alpha}\cdot\vec{c})}. \tag{31}$$

Note that r_{min} is not the minimum distance from the CM to an *element* of the COR locus; that distance is zero. r_{min} is the minimum distance from the CM to the *boundary* of the COR locus. r_{min} is indicated in figure 5-5.

It will also be useful to have the angles at which the COR locus boundary intersects the disk boundary. From equation 30 we obtain

$$\cos\eta_{r=a} = \frac{((\vec{\alpha}\cdot\vec{c})^2 + 4a^2)^{1/2} - (\vec{\alpha}\cdot\vec{c})}{2a} \tag{32}$$

5.1.2. Curvature of the COR Locus Boundary at r_{min}

From equation 29 we can find the curvature of the COR locus boundary at r_{min}:

$$\frac{d^2r}{d\varepsilon^2} = \frac{2a^2(\vec{\alpha}\cdot\vec{c})((\vec{\alpha}\cdot\vec{c})^2 + 2a(\vec{\alpha}\cdot\vec{c}) + 2a^2)}{((\vec{\alpha}\cdot\vec{c}) + 2a)^4} \tag{33}$$

which is equivalent to a radius of curvature of

$$s = \frac{a(\vec{\alpha}\cdot\vec{c})((\vec{\alpha}\cdot\vec{c}) + 2a)^2}{(\vec{\alpha}\cdot\vec{c})^3 + 4a(\vec{\alpha}\cdot\vec{c})^2 + 8a^2(\vec{\alpha}\cdot\vec{c}) + 4a^3}. \tag{34}$$

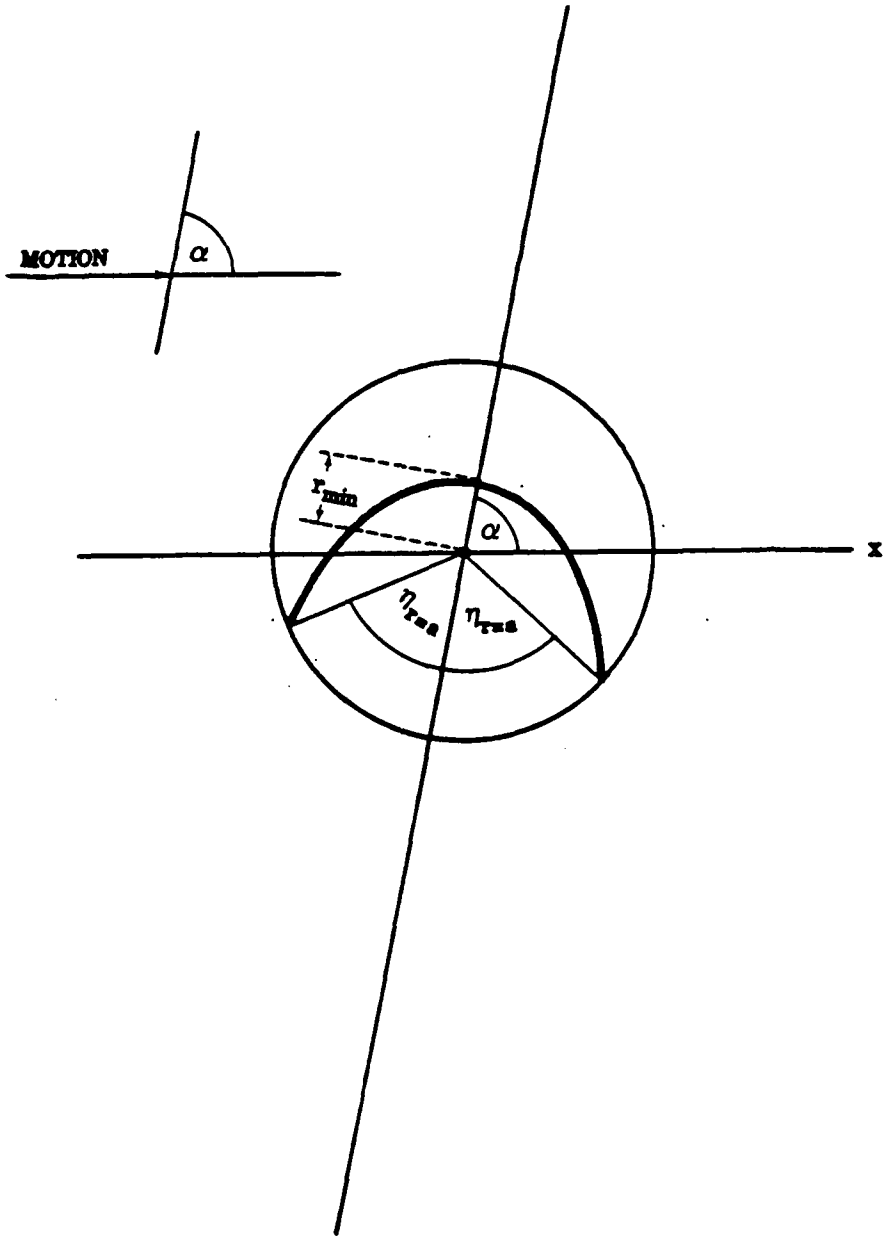

Figure 5-5: COR locus boundary for $r < a$

5.2. |COR| > a

If $r > a$, we cannot find a simple equation analogous to equation 25 constraining $\vec{q}_r$ to the boundary of $\{\vec{q}_r\}$. An effective approach is to parametrize the boundary of the $\{\vec{q}_r\}$ locus by the angle ω of equation 21, and solve for both ε and r by binary search.

For each ω the following procedure is used: We guess a value of r, in the range $a < r < r_{tip}$, where r_{tip} is an upper bound to be found in section 5.2.1. Equation 21 is then used to calculate a value of $\vec{q}_r$. Angle η is related to the terms of equation 21 by

$$\eta = \arctan \frac{-\vec{v}_x}{\vec{v}_y} \tag{35}$$

and so can be computed from ω. Equation 23 can be written in terms of the angle η as

$$r^2 = |\vec{q}_r| \, (\vec{\alpha} \cdot \vec{c} + r \cos \eta) \tag{36}$$

which is easily tested. If it is satisfied, we have found angle η and magnitude r describing a point on the boundary of the COR locus. ε is then obtained from η using equation 24.

If the left-hand side of equation 36 is greater (resp. less) than the right-hand side, we increase (resp. decrease) the value of r guessed above. In this way we perform a binary search, quickly converging on a solution for r and ε.

Figure 5-6 shows the boundary of the COR locus for various $\vec{c}$ and α. The part of the boundary inside the disk was computed using equation 30, while the part outside the disk was found by binary search as outlined here. Calculation of each locus required about 2 CPU seconds on a VAX-780.

5.2.1. Tip Line

We can calculate the extremum of the COR locus analytically. For many purposes this may be all that is required. Additionally, it gives us a range within which to conduct the binary search discussed in section 5.2. By symmetry, r takes on an extremal value when $\eta = 0$. In figure 4-6 this corresponds to $\vec{v}_x = 0$, which in turn occurs only when $\omega = 0$ or $\omega = \frac{\pi}{2}$.

At $\omega = 0$ we find from equation 21

$$\vec{q}_r = \vec{\alpha} \, r \, . \tag{37}$$

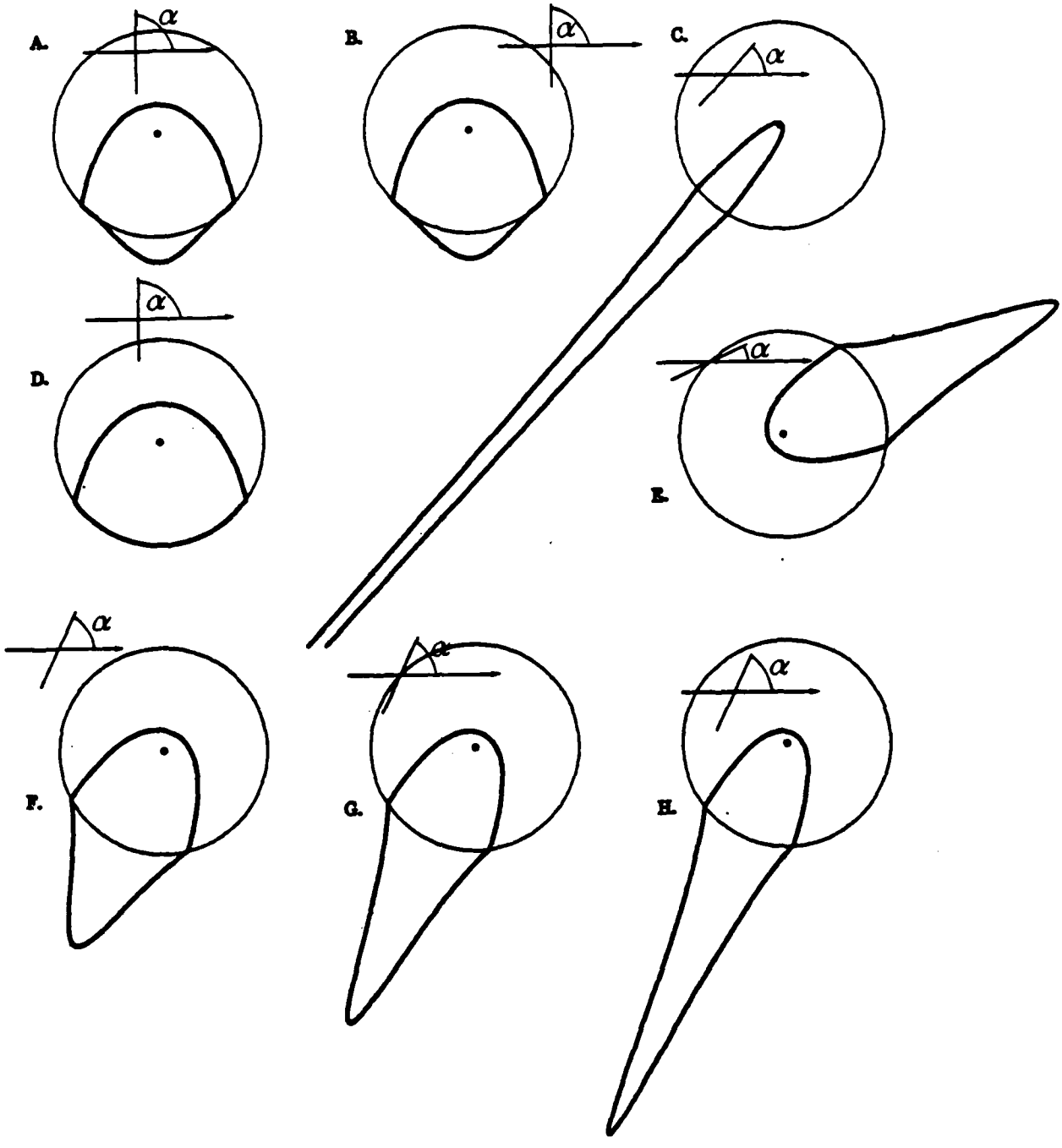

Figure 5-6: Boundaries of COR loci for various $\vec{c}$ and α

Substituting this into equation 23 we obtain

$$r = \frac{\vec{\alpha}\cdot\vec{c}}{2}. \tag{38}$$

This extremum has no apparent meaning.

At $\omega = \frac{\pi}{2}$ we find from equation 21

$$\vec{q}_r = \vec{\alpha}\frac{r^3}{r^2 + a^2}. \tag{39}$$

At this value equation 23 yields

$$r_{tip} = \frac{a^2}{\vec{\alpha}\cdot\vec{c}} \tag{40}$$

This is the greatest distance $\vec{r}$ may be from the CM, and it occurs at polar angle $\varepsilon = \pi + \alpha$. In figure 5-7 we plot r_{tip} vs. contact angle α, for a given value of $\vec{c}$. As α is varied, the tip of the COR locus at distance r_{tip} from the CM traces out straight line, the *tip line*.

The use of this graphical construction is illustrated in figure 5-7. For a given value of α, as shown, r_{tip} is at the intersection of the tip line described above with a ray from the CM at angle $\pi + \alpha$.

An interesting case occurs when $\vec{\alpha}$ becomes perpendicular to $\vec{c}$. (Note that this does not require $\alpha = \frac{\pi}{2}$.) As $\vec{\alpha}\cdot\vec{c} \rightarrow 0$, we have $r_{tip} \rightarrow \infty$. The COR at infinity corresponds to pure translation perpendicular to $\vec{a}$.

Mason (Mason, 1985) showed that if $\vec{\alpha}\cdot\vec{c} = 0$, pure translation is assured. In that case the *entire* COR locus (not just its farthest point) must go to infinity. In all other cases $\vec{\alpha}\cdot\vec{c} \neq 0$, and the CM (for one) remains in the COR locus. Figure 5-6c shows a case in which $\vec{\alpha}$ is almost perpendicular to $\vec{c}$, illustrating the transition from a COR locus entirely at infinity to one which includes the CM.

We now have the ability to quickly compute the COR locus for any $\vec{c}$ and α.

5.2.2. Curvature of the COR Locus Bound at the Tip

The radius of curvature of the COR locus boundary at the tip can be found analytically, and will prove useful.

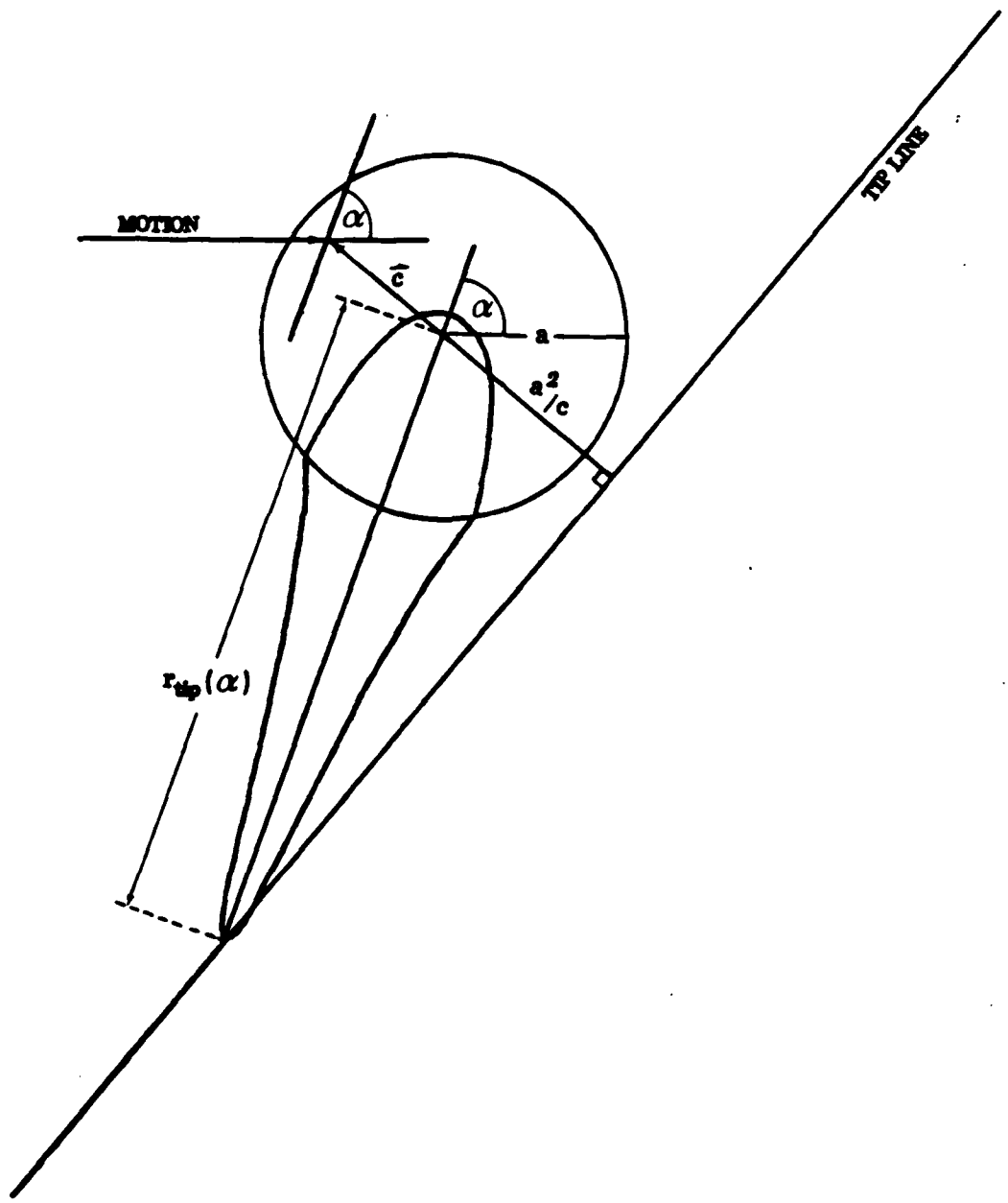

Figure 5-7: $r_{tip}(\alpha)$ vs. α, and construction of the tip line

From equations 21 and 35 we compute taylor expansions for η and $\vec{q}_r$ to lowest order ω^2, at $\omega = \frac{\pi}{2}$. The expansions are substituted into equation 36, and the result expanded about $\omega = \frac{\pi}{2}$ to lowest order ω^2. Finally we expand about $r = r_{tip}$ to order r^1.

We find

$$\frac{d^2r}{d\varepsilon^2} = r_{tip}\left(\frac{1}{2} - \frac{r_{tip}^4}{a^4}\right) \tag{41}$$

which corresponds to a radius of curvature

$$s = \frac{r_{tip}}{\frac{1}{2} + \frac{r_{tip}^4}{a^4}}. \tag{42}$$

5.3. Summary

In this section we have found the boundary of the COR locus for any choice of $\vec{c}$ and α. Within the disk the boundary is given by a simple formula relating r and ε, the polar coordinates of the boundary (equation 30). Outside of the disk, the polar coordinates of the boundary are found by binary search as outlined in section 5.2. We have found the minimum and maximum distances from the CM to the boundary (r_{min} and r_{tip}), and the curvature of the boundary at those points. And we have found the polar angles at which the boundary of the COR locus intersects the boundary of the disk (equation 32).

6. Applications

A useful application of the results found above is to the problem of aligning an object by pushing it. In figure 1-2 a misoriented rectangle is being pushed by a fence. The fence is moving in a direction perpendicular to its front edge. Evi..ly the rectangle will rotate CW as the fence advances (Mason, 1985), and will cease to rotate when the edge of the rectangle comes into contact with the front edge of the fence (Brost, 1985). The problem is to find how far the fence must advance to assure that the CW motion is complete.

The geometry of this problem differs from the geometry used in previous sections. Previously a point pusher made contact with a straight object edge. Here the straight edge of the pusher makes contact with a point (corner) of the object. But since the coefficient of friction between the pusher and the

edge of the object (μ_c) is zero, we know that in either case the force exerted by the pusher on the object is normal to the edge, regardless of whether the edge is that of the pusher or that of the object.

Since the motion of the object can depend only on the force applied to it, the angle of the fence takes the place of the angle of the object edge (α), and all the results derived above remain unchanged.

In this section we will generalize the problem slightly, relative to the problem illustrated in figure 1-2:

- The object pushed is arbitrary, not a rectangle.
- The motion of the fence is not necessarily perpendicular to its face.

First we circumscribe a disk of radius *a* about the object. The disk is centered at the CM of the object (figure 6-1). Note that the contact point need not be on the perimeter of circumscribed disk.

We know (Mason, 1985) that the object will rotate CW, and will cease to rotate when the final configuration shown in figure 6-2 is reached.

We now ask the rate of rotation of the object about the COR, with unit advance of the pusher. Let the angle of the CM from the direction of motion of the pusher be β. This is also the angle between the tip line and the perpendicular to the line of motion. (Both angles are indicated in figure 6-1). We have

$$dx = y\, d\beta \tag{43}$$

where y is the distance from the line of motion to the COR. To find the minimum rate of rotation we must find the maximum value of y for any COR in the COR locus.

Figures 6-1 and 6-2 also show the COR loci for the pushed disk. The COR furthest from the line of motion is at point A in figure 6-2 . The tip of the COR locus is at point B. The maximum value of y for any COR in the locus is the distance from the line of motion to point A. It is well approximated by the vertical distance from the line of motion to point B. We will first solve the fence-push problem using this approximation, and then bound the difference between the answer thus obtained and the exact answer.

From figure 6-3 we find

$$y_{approx} = c \sin\beta + r_{tip} \sin\alpha \tag{44}$$

$$\text{where } r_{tip} = \frac{-a^2}{c\cos(\alpha+\beta)}.$$

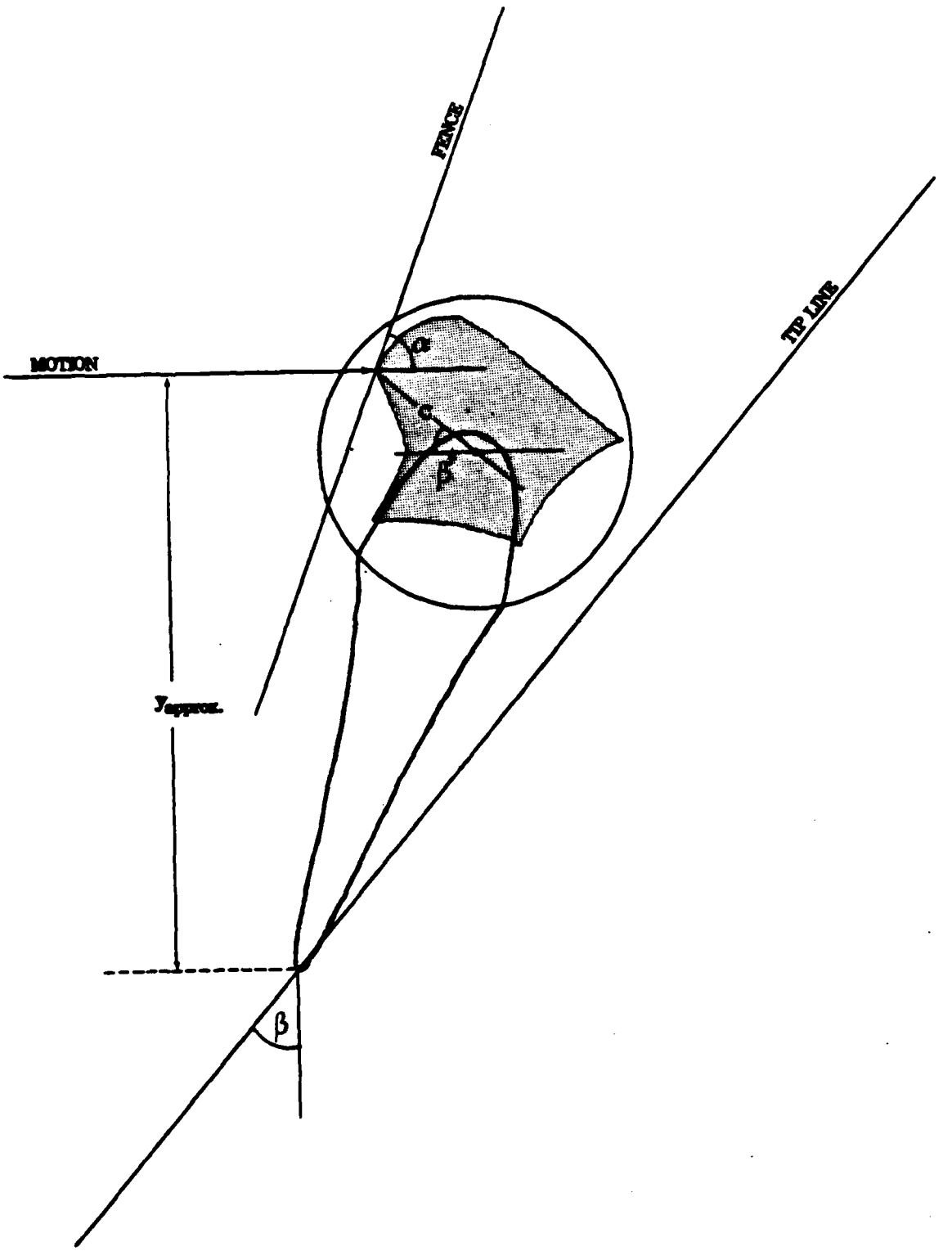

Figure 6-1: Initial configuration of object and fence, and resulting COR locus

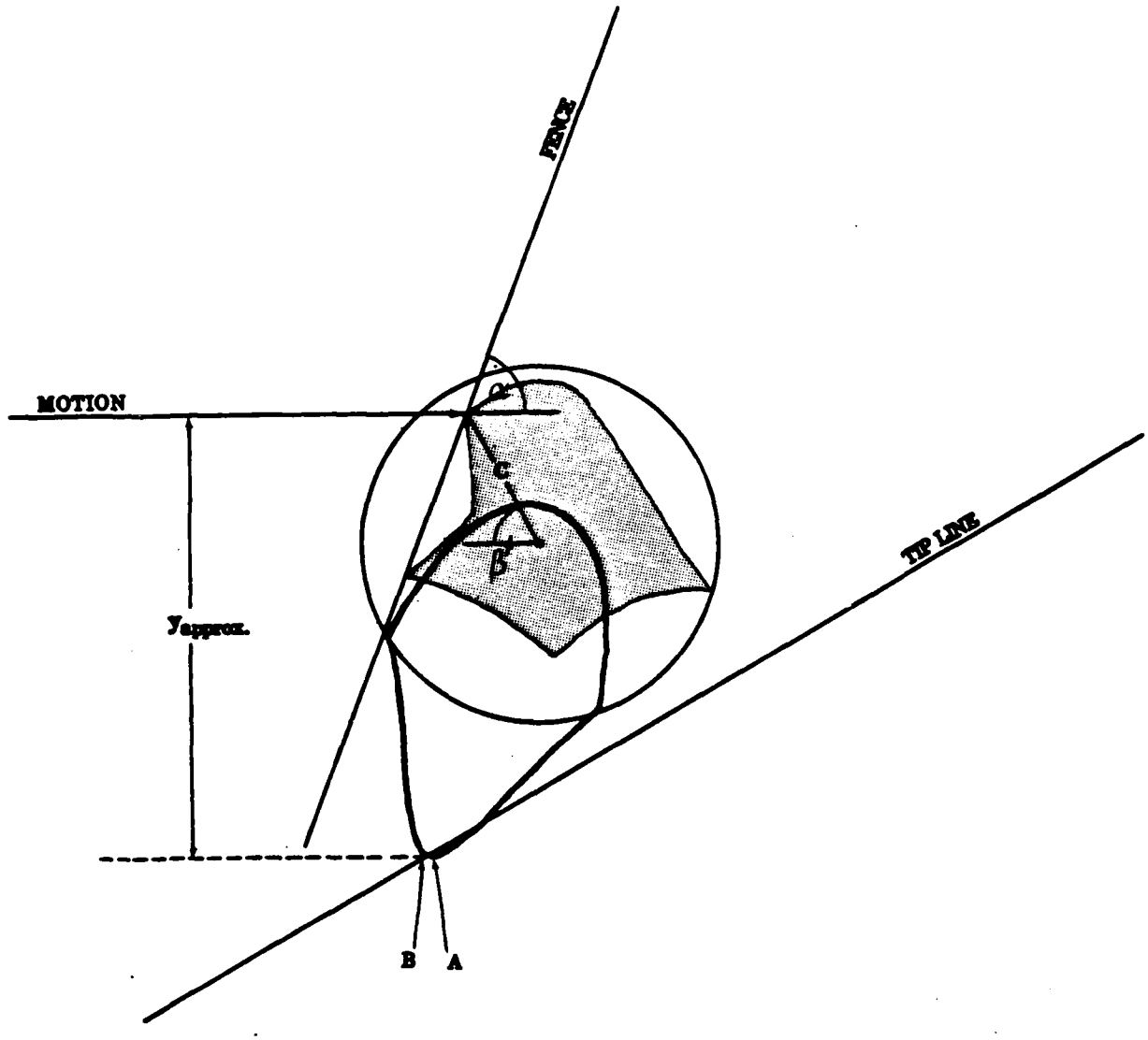

Figure 6-2: Final configuration of object and fence, and resulting COR locus

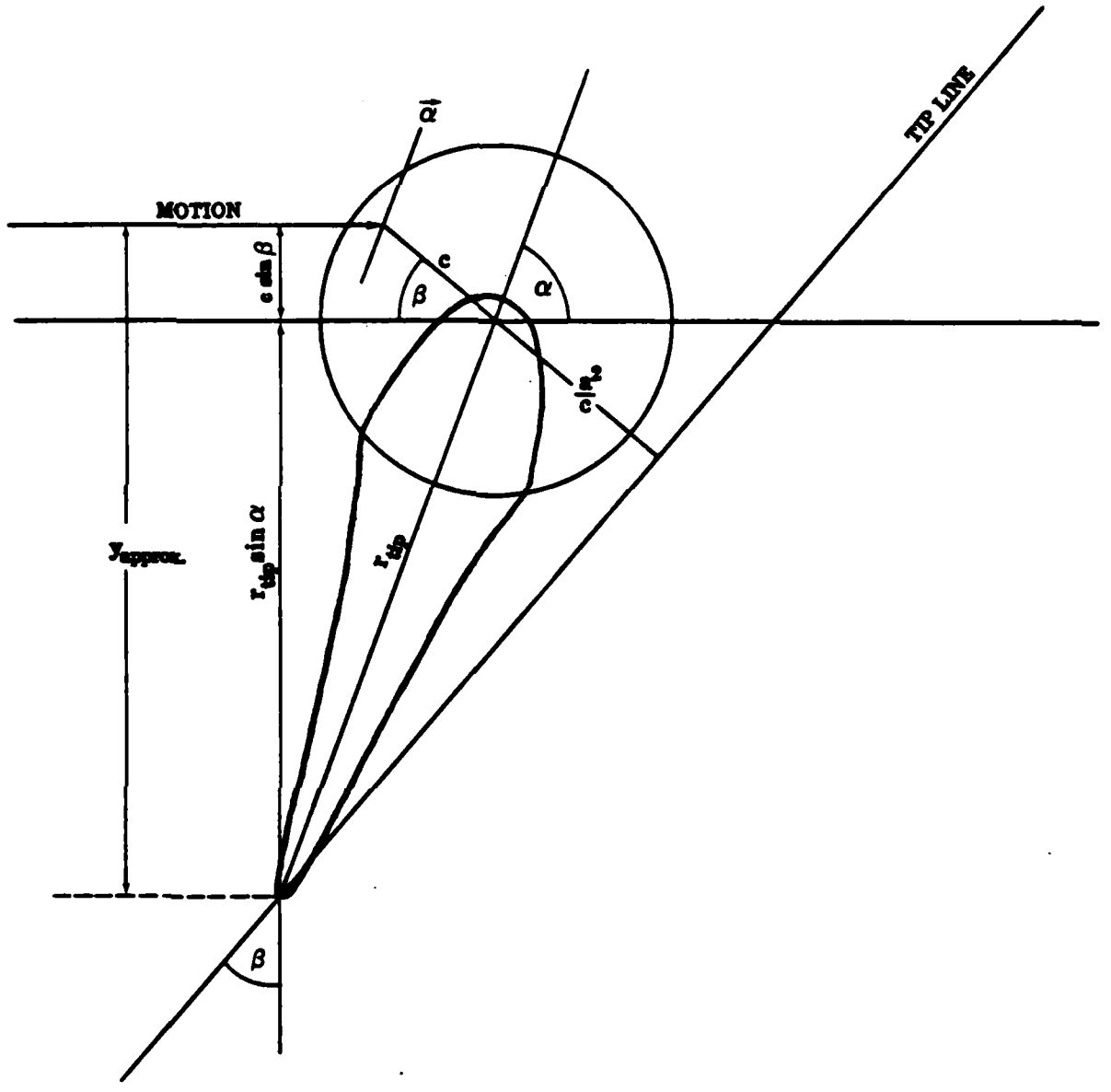

Figure 6-3: y_{approx} is the distance from the line of motion to the tip of the COR locus

We can now integrate $dx = y\ d\beta$ to obtain the indefinite integral

$$x = -c\cos\beta - \frac{a^2\sin\alpha}{2c}\log\left|\frac{1+\sin(\alpha+\beta)}{1-\sin(\alpha+\beta)}\right|. \tag{45}$$

To find the maximum pushing distance, Δx, required to cause the object to rotate from its initial configuration shown in figure 6-1 to its final configuration shown in figure 6-2, we simply substitute the initial and final values of β into equation 45, and take the difference $x_{final} - x_{initial}$

The value of y used (equation 44) is slightly less than the true maximum distance from the line of motion to any point of the COR locus. Using the construction of figure 6-4 we can approximate the true distance y from the line of motion to the lowest point of the COR locus (point A):

$$y_{true} = c\sin\beta + (r_{tip} - s)\sin\alpha + s \tag{46}$$

Inserting the radius of curvature s from equation 42 in equation 46, we find that $dx = y\ d\beta$ cannot be integrated in closed form. However if we make the approximation

$$s = \frac{r_{tip}}{\frac{1}{2}+\frac{r_{tip}^4}{a^4}} \approx \frac{a^4}{r_{tip}^3} \tag{47}$$

then $dx = y\ d\beta$ can be integrated to yield an additional required pushing distance of

$$x_{adnl} = \frac{-c^3}{a^2}(1-\sin\alpha)\left(\sin(\alpha+\beta) - \frac{\sin^3(\alpha+\beta)}{3}\right). \tag{48}$$

The approximation made in equation 42 slightly *overestimates* the radius of curvature s, leading to a slight overestimate of y_{true}, and therefore to a upper bound for the required additional pushing distance x_{adnl}

The sum of equations 45 and 48 therefore provides an upper bound for the required pushing distance. For most purposes equation 45 alone will suffice.

In the case of figures 6-1 and 6-2, if the disk diameter is a, we have $\alpha = 70$ degrees, $c = .8125\,a$, $\beta_{initial} = 40$ degrees, and $\beta_{final} = 60$ degrees. equation 45 yields a required pushing distance of $1.0543\,a$, and equation 48 yields an additional distance of $.0015\,a$.

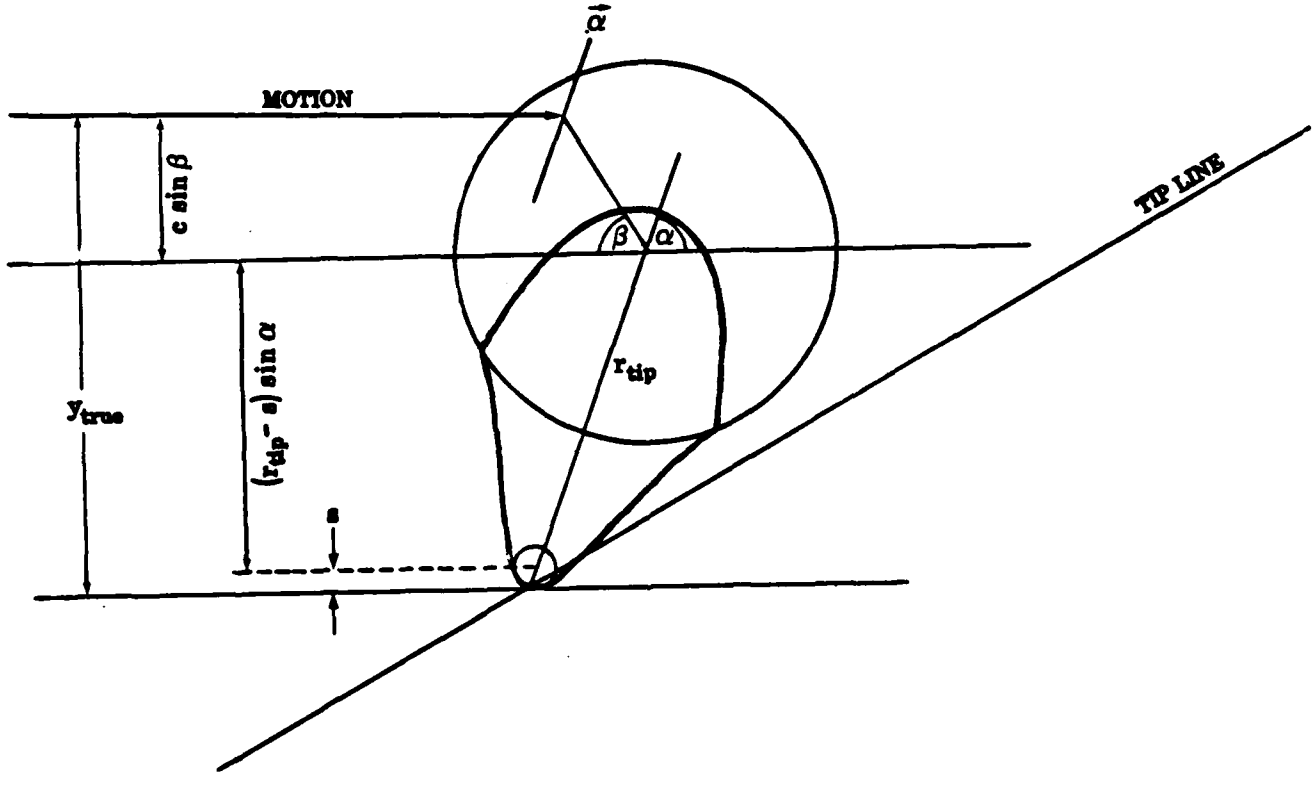

Figure 6-4: y_{true} is a bound for the distance from the line of motion to the true lowest point

7. Conclusion

We have found the locus of all possible centers of rotation for a pushed object sliding on a level surface. A major assumption is the neglect of friction at the point of contact between the pusher and the object. A forthcoming paper will show how the effect of such friction can be calculated. It will not be necessary to modify the derivations above to incorporate friction.

Another major assumption is that the support force distribution is confined to a disk. The loci found above are exact bounds on the center of rotation of a disk with an arbitrary distribution of support forces. For objects other than disks, the loci found above are outer bounds on the center of rotation, but tighter bounds are possible.

An immediate application of the results derived here is to the problem of the distance a sliding object must be pushed by a fence before it rotates into alignment with the fence. This problem requires us to find the *slowest* possible rotation of the sliding object.

One application of the *fastest* possible rotation would be to find the maximum misalignment of an object when it is pushed from a known configuration.

Another possible application is the calculation of the maximum torque a grasp can withstand before the grasped object slips. Just as the support force distribution is unknown in the sliding problem treated above, the distribution of pressure exerted by a gripper on a grasped object is unknown. It may be possible to use similar methods to find the strength of the grasp.

8. Acknowledgements

We wish to acknowledge useful discussions with Randy Brost and with Matt Mason. We especially thank Randy Brost for several readings of this paper, and for many suggestions. Figure 1-1 was copied from (Mason, 1985). Several equations were obtained or simplified using MACSYMA.

9. Appendix - Validity of Energy Minimization

Some question has arisen about the validity of the assumption that the system will rotate about a COR which minimizes the frictional energy loss. (The assumption is known to be valid in conservative systems, but the presence of friction makes the sliding system dissipative.) Here we show that the same equation which is obtained from energy minimization (equation 8, 12, 22, or 23) can also be

obtained from a straightforward application of Newton's laws.

Since the sliding system is assumed to be quasi-static, we have zero acceleration, and Newton's laws simply require total force and total torque to be zero. In other words the applied force and torque due to the pusher must be opposed by an equal and opposite force or torque created by frictional forces between the object and the surface it is sliding on.

Since the coefficient of friction at the pusher/object contact is zero, the applied force is directed perpendicular to $\vec{\alpha}$. Torque may be measured with respect to any origin. We choose to measure it about the COR. Denoting the applied force $\vec{F}_A$, the torque is

$$\tau_r = |\vec{F}_A \times (\vec{c} - \vec{r})| = |\vec{F}_A| \; \vec{\alpha} \cdot (\vec{c} - \vec{r}) . \tag{49}$$

The opposing torque developed by frictional forces is

$$\tau_r = \mu_s \int S(\vec{w}) \, |\vec{w} - \vec{r}| \, d\vec{w}. \tag{50}$$

Setting the opposing torques equal we can solve for the applied force

$$|\vec{F}_A| = \frac{\mu_s}{\vec{\alpha} \cdot (\vec{c} - \vec{r})} \int S(\vec{w}) \, |\vec{w} - \vec{r}| \, d\vec{w}. \tag{51}$$

We also require translational forces to cancel:

$$\vec{F}_A = - \int F(\vec{w}) d\vec{w} \tag{52}$$

where we know that $\vec{F}(\vec{w})$, the element of frictional force at $\vec{w}$, must be directed opposite to the direction of motion at $\vec{w}$. The direction of motion at $\vec{w}$ is perpendicular to the vector $(\vec{w} - \vec{r})$, where $\vec{r}$ is the COR. The magnitude of the element of frictional force at $\vec{w}$ is $\mu_s \, S(\vec{w})$. So we have

$$\vec{F}(\vec{w}) = \mu_s \, S(\vec{w}) \left[\frac{-(\vec{w} - \vec{r})_y \, \vec{x}}{|\vec{w} - \vec{r}|} + \frac{(\vec{w} - \vec{r})_x \, \vec{y}}{|\vec{w} - \vec{r}|} \right]. \tag{53}$$

Integrating over all $d\vec{w}$

$$\vec{F}_A = - \mu_s \int S(\vec{w}) \left[\frac{-(\vec{w} - \vec{r})_y \vec{x}}{|\vec{w} - \vec{r}|} + \frac{(\vec{w} - \vec{r})_x \vec{y}}{|\vec{w} - \vec{r}|} \right] d\vec{w}. \tag{54}$$

We also know that the applied force $\vec{F}_A$ is perpendicular to $\vec{\alpha}$, so

$$\vec{F}_A = |\vec{F}_A|(-\alpha_x \vec{y} + \alpha_y \vec{x}). \tag{55}$$

Formally exchanging $\vec{x}$ with $\vec{y}$, and equating the right-hand-sides of equations 54 and 55 we have

$$|\vec{F}_A|\,\vec{\alpha} = \mu_s \int S(\vec{w}) \frac{\vec{w} - \vec{r}}{|\vec{w} - \vec{r}|}\, d\vec{w}. \tag{56}$$

Combining the result from consideration of total torque (equation 51) with the result from consideration of total translational force (equation 56) yields

$$\frac{\vec{\alpha}}{\vec{\alpha}\cdot(\vec{c} - \vec{r})} \int S(\vec{w})\,|\vec{w} - \vec{r}\,|\, d\vec{w} = \int S(\vec{w}) \frac{\vec{w} - \vec{r}}{|\vec{w} - \vec{r}|}\, d\vec{w} \tag{57}$$

which can be cast in a form equivalent to equation 8:

$$d_r\,\vec{\alpha} = \vec{v}_r\,\vec{\alpha}\cdot(\vec{c} - \vec{r}) \tag{58}$$

where

$$d_r = \int S(\vec{w})\,|\vec{w} - \vec{r}\,|\, d\vec{w}$$

and

$$\vec{v}_r = \int S(\vec{w}) \frac{\vec{w} - \vec{r}}{|\vec{w} - \vec{r}|} d\vec{w}.$$

References

Brost, Randy. *Planning Robot Grasping Motions in the Presence of Uncertainty.* Technical Report CMU-RI-TR-85-12, Carnegie-Mellon University, 1985.

Mani, Murali and W.R.D. Wilson. *A Programmable Orienting System for Flat Parts.* NAMRII XIII, 1985.

Mason, Matthew T., J. K. Salisbury. *Robot Hands and the Mechanics of Manipulation.* The MIT Press, 1985.

Pingle, K., Paul, R., Bolles, R. Programmable Assembly, three short examples. Film, Stanford AI Lab, 1974.

Prescott, J. *Mechanics of Particles and Rigid Bodies.* Longmans, Green and Co., London, 1923.

END

FILMED

1-86

DTIC